The Paton WELDING JOURNAL

July 2000 # 7

English translation of the monthly «Avtomaticheskaya Svarka» journal published in Russian since 1948

Editor-in-Chief B.E. Paton

Editorial board:

Yu.S.Borisov V.F.Grabin
Yu.Ya.Gretskii A.Ya.Ishchenko
V.F.Khorunov
S.I.Kuchuk-Yatsenko
Yu.N.Lankin V.K.Lebedev
V.N.Lipodaev L.M.Lobanov
V.I.Makhnenko A.A.Mazur
L.P.Mojsov V.F.Moshkin
O.K.Nazarenko V.V.Peshkov
I.K.Pokhodnya I.A.Ryabtsev
V.K.Sheleg Yu.A.Sterenbogen
V.I.Trufiakov N.M.Voropai
K.A.Yushchenko V.N.Zamkov
A.T.Zelnichenko

«The Paton Welding Journal» monthly is published by the E.O. Paton Electric Welding Institute of the National Academy of Sciences of Ukraine with the support rendered by the International Association «Welding».

Promotion group:
V.N.Lipodaev, V.I.Lokteva
A.T.Zelnichenko (Exec. director)
Translators:
S.A.Fomina, I.N.Kutianova, T.K.Vasilenko
Editorial and advertising offices are located at PWI, Dept. 51, 11, Bozhenko str., 03680, Kyiv, Ukraine.
Tel.: (38044) 227 67 57
Fax: (38044) 268 04 86
E-mail: paton@i.kiev.ua

Subscriptions:
$460, 12 issues

«The Paton Welding Journal» Website:
http://www.nas.gov.ua/pwj

CONTENTS

© The E.O. Paton Electric Welding Institute of the National Academy of Sciences of Ukraine, 2000

Науково-технічна бібліотека ІЕЗ ім. Є.О. Патона Інв. №

AGEING AND PROCEDURE OF EVALUATION OF THE STATE OF METAL OF THE MAIN PIPELINES IN SERVICE

B.E. PATON[1], **S.E. SEMENOV**[1], **A.A. RYBAKOV**[1], **S.K. VASILENKO**[2] and **V.M. VASILYUK**[3]
[1]The E.O. Paton Electric Welding Institute, NASU, Kyiv, Ukraine
[2]GAO Pridneprovsk Main Pipelines, Kremenchug, Ukraine
[3]GAO «Druzhba» Main Pipelines, Lvov, Ukraine

ABSTRACT

Basic concepts of ageing of metal of the line pipelines in use for a long time are formulated proceeding from up-to-date knowledge and available experimental data. The principles of classification of the state of the pipeline materials, allowing for the service effects, are suggested.

Key words: *pipeline, service, material, state, ageing, residual properties, methodology, classification.*

Various aspects of the problem of metal ageing in operating main pipelines have been rather extensively discussed over the last years. In this connection, the possibility of a long-term accident-free operation of such constructions raises certain doubts. The importance of the above problem reaches far beyond the interests of individual enterprises of the oil and gas industry. Incorrect evaluation of the role of metal ageing processes is fraught with tremendous material and financial losses, as well as ecological disasters, to say nothing of the possible irreparable consequences. Considering the ramified network of the main oil and gas pipelines which is characteristic of the European regions, the highly critical condition of the old pipelines can result in grave crisis phenomena in economy. In view of the limited financial resources of the countries with the transition economy, the need for renovation and, especially, for construction of the new pipelines, creates great difficulties. All this directly concerns the system of the main pipelines of Ukraine.

A thorough analysis of the metal ageing processes is required in evaluation of the reliability characteristics of pipelines which have been in operation for a long time. Precise criteria are needed which would permit creating the company's strategy with regard to extension of the service life and rehabilitation of the pipelines in service.

Proceeding from analysis of publications and the results of the authors' own investigations, this paper formulates the basic statements concerning the influence of the ageing processes on the pipe metal. A classification approach to evaluation of the state of materials of the pipelines in service allowing for the ageing phenomenon, is described.

In current technical publications, ageing of metal of the main pipelines is considered in terms of the processes of their wear and degradation [1, 2]. The «ageing» term is interpreted rather broadly: it covers the description of phenomena which characterize changes in the materials related to the structure age, including those developing under the influence of service impacts. Widening of the limits of interpretation of the nature of metal ageing is also promoted by development of the concepts of the processes leading to pipeline failures as a result of cracking, corrosion-mechanical and other fractures. The phenomena inherent in the metal ageing are quire diverse. The developing predecomposition processes and decomposition of oversaturated solid solutions proper or change of structural states after mechanical deformation can be considered among them. Ageing is accompanied by precipitation of disperse particles of new phases, intercrystalline zone enrichment with impurity atoms and heterophase nature of local zones. Ageing can result in changes on the substructural level related to defect accumulation, increase and plastic relaxation of inner microstresses. Lowering of grain boundary strength under the impact of hydrogen, etc. are also regarded as the ageing phenomena.

Embrittlement or fracture, including cracking of the old pipeline metal, is primarily related to strain ageing, damage at repeated-static loads and impact of aggressive media [3 – 11, etc.]. The above mechanisms lead to a higher susceptibility of steel to cracking and brittle fracture as the steel brittleness temperature shifts towards the pipeline operational temperature.

O.I. Steklov, for instance, notes [4] that the structure and properties of the metal in service change in time compared to its initial characteristics under the influence of corrosive media,

© B.E. PATON, S.E. SEMENOV, A.A. RYBAKOV, S.K. VASILENKO and V.M. VASILYUK, 2000

temperature fluctuations, working loads. Here, the structure change is primarily related to the steel matrix substructure. Change of the mechanical properties is accompanied by an increase in the strength values (HB, σ_t, σ_y), lowering of toughness and ductility characteristics (δ_5, ψ) and of brittle fracture resistance characteristics (KCU, KCV, K_c).

Thus, the concept of the detrimental influence of the factors of long-term service on the pipeline material is being developed currently. Proceeding from that conclusions are made of the metal performance deterioration with time and increase of the probability of pipeline accidents. In connection with the possible degradation of the material the limit fatigue life of the pipelines is estimated to be 40 to 80 years of service [12].

In a number of papers attention is given to the hazard of an essential degradation of the material properties directly during the planned periods of pipeline operation. Investigation of a number of pipe metal samples showed that the indications of the initial stage of strain ageing are found already after a relatively short-time exposure to the load of up to 5 years [11]. The authors [11, 13, 14] believe that irrespective of the alloying system and the level of pipe steel strength, two time intervals can be signed out in the dependence of the mechanical properties of the base metal or welded joints on time. In the first interval, the ductile and tough properties of the metal change but little, while the number of failures is minimal. In the second interval, the characteristics of ductility and toughness decrease and the number of pipeline fai-lures rises. The limit time separating the above two intervals, is tentatively equal to 10 to 12 years of pipeline operation. The following data are given in the references cited by us. After 20 years of the pipeline service, the weld metal reduction in area decreases by 25 %, and that of the pipe base metal (17GS steel) by 30 %. The impact toughness of steel drops to 20 J/cm^2, this being lower than the standard requirements to the material. The authors of [13] state that a change of the mechanism of microfracture from the tough to the brittle mode is observed in transition from the first to the second interval. At maximal length of the operational period the material can become completely embrittled.

It is obvious that the abrupt drop of impact toughness in the second time interval is manifested against the background of its high values (of the order of 200 J/cm^2), given by the authors for the material initial condition. However, the values of impact toughness of steel in the initial condition, given in the cited studies, do not seem to be quite correct to us. The levels of impact toughness of the metal of pipes produced about 30 years ago, were much lower, which is indicated, for instance, by the data of [15], [16].

Other researchers [2, 3, 17, 18], while noting a deterioration of the ductility and toughness characteristics of the pipe metal after long-term service, do not focus on the critical time periods during which the material properties can abruptly change.

In [12] it is pointed out that under the conditions of service at the climatic temperatures, the pipe steel properties change but slightly: σ_t, σ_y, S_c by up to 10 %; δ_5, ψ in the range of 15 to 20 %. The level of residual stresses (in the absence of plastic deformations) also changes insignificantly (< 15 %). The parameters characterizing the properties of locally embrittled zones, change considerably depending on the duration of service. As a result of ageing, especially in case of hydrogenation of steel, the brittle fracture resistance changes to a greater extent, than the standard mechanical properties.

The conclusion on the relatively slight change of the pipe metal mechanical properties, can be made when analyzing the data of [19] from which it follows that the characteristics of the mechanical properties of the studied pipe metal completely meet the standard requirements after 25 to 30 years of operation. After a long period of ope-ration, the pipe material preserved a comparatively good plastic deformability under the conditions of hydraulic testing to fracture, whereas the inner pressure at rupture was essentially higher than that achieved at the start of the pipe metal yield.

The results of our testing of pipe metal samples cut out of Ukrainian PDMN and «Druzhba» companies' oil pipelines which had run for 20 to 35 years, are of interest. Testing of materials (base metal, factory and field welded joints) did not reveal any phenomena characteristic of advanced stages of ageing. Extensive testing (in these cases many samples of pipe metal were studied, namely locally produced steels of grades 20, 19G, 14GN, 17GS, 10G2S1, 14KhGS and foreign variants of steel produced in Czechia and France) did not reveal any intergranular fracture which would point to hydrogen embrittlement or a significant heterogeneity (heterophase nature) of intercrystalline junction zones.

In the studied samples of materials no essential changes of the mechanical properties (including crack and microcleavage resistance characteristics) under the influence of service factors were found either, while the observed deviation of individual parameters from the standard values can be safely attributed to the structural features of the initial steels and imperfection of the technologies during their fabrication.

In hydraulic testing of a section abutted of coils with considerable dents, failure occurred at the stress on the level of the steel ultimate strength after the pipe perimeter in the fracture zone increased by more than 3 %. The site of fracture which was of a tough nature, was on the coil of 14GN steel in the base metal at a distance from the

Table 1. Relative number of pipeline failures because of defects and damage of the metal, %

Reference	Years of service					
	0 – 5	5 – 10	11 – 15	15 – 20	20 – 30	30 – 35
[14]	10.0	11.0	11.0	1.0	1.0	0
[15]	7.7	10.2	5.7	0	0	0

zone of the dent location, as well as the factory and the circumferential joints.

Thus, under the conditions of long-term (up to 35 years) operation, the material of the studied oil pipelines did not undergo any significant and often even slight changes of the service properties and, therefore, preserved the required performance. In this case, for the long-time loaded carrying elements of the pipeline which the steel pipes and the welded joints are, the characteristic processes of strain ageing were accompanied by a gradual formation of the substructure, and a certain increase in the dislocation density promoting metal strengthening, did not create any critical conditions prone to cracking, due to the processes of plastic relaxation of inner microstresses.

Based on the statistics of the main pipeline failures [1, 11, 13 – 15, etc.], it is also rather difficult to make unambiguous conclusions on the influence of the ageing factor on the material performance.

In analysis of the data on pipeline failures in connection with the time factors, it has to be taken into account that statistical processing, despite a seemingly extensive data bulk, is performed in the field of rather dissimilar information. Over an almost half a century long period of pipeline transportation development in FSU and CIS countries, significant changes have taken place in the range of the pipe grades and sizes, materials and technologies used, pipeline service conditions, etc.

The results of statistical processing largely depend on the «quality» of the initial data. Experience shows that pipeline failures, as a rule, develop through a number of different causes in each concrete case. Revealing by statistical methods the role of a particular factor which promotes failure initiation, requires a thorough selection of the initial data, which involves considerable difficulties, if analysis is performed based on the acts of initial investigation of the causes for the failures. A detailed investigation of the failure causes is conducted by far not in all the cases, which does not eliminate errors or misinterpretation of the initial information.

By the data of [2], the dependence of the intensity of failures of the main oil pipelines on the duration of their operation, is characterized by the periods of running-in, normal operation and wear. During running-in the failures are due to structural defects in the pipes and poor performance of the construction and erection work. During normal operation, the intensity of failures is minimal, and practically constant. During the wear period, the intensity of pipeline failures increases, this, in the opinion of the author, being due to ageing (degradation) of the material of the load-carrying steel pipe, as well as metal corrosion, abrasive-corrosion failures of the inner surface, and stress corrosion failures.

There is no doubt of the influence of the corrosion factor. However, the role of metal ageing (meaning, at least the influence of force loading) in the increase of the number of pipeline failures with time, is not as obvious. With the period of operation of 10 to 15 years, an abrupt rise in the number of gas pipeline failures up to 32 % of their total number is found [13, 14]. This, in the opinion of the authors of the earlier mentioned studies, confirms the influence of the found by them degradation of the material mechanical properties in the above time period on the failure processes. However, from the initial information given in [15] it follows that the majority of failures in the found spike are the failures due to hydrogen sulfide corrosion and inner erosion of metal (21.3 %). The above specific cause for the fractures in a certain group of gas pipelines in 1970s can hardly characterize the regularities of the change of the state of materials of other gas pipeline systems.

The data of [14, 15] on pipeline rupture because of pipe defects, field butt joint defects and metal damage in transportation of pipes and pipeline construction, depending on the time of their service (Table 1) do not confirm the opinion of the increase in the number of ruptures after 11 to 15 years of service as a result of lowering of the metal ductility and toughness characteristics.

As a result of analysis of VNIPItransgas information on failures of Ukrainian gas pipelines, performed by us allowing for the number N of the objects of observation (gas pipelines), in each time interval of their service, it was found (Figure) that the relative number of failures n/N (n is number of failures) is little dependent on the period of the pipeline operation.

Naturally, it does not follow from the given data that metal damage related to the ageing process, does not have a noticeable influence on the formation of fracture sites. A different mechanism can be assumed. It is obvious that the changes in the material proceeding under the influence of service impacts, turned out to be not so significant as to have an essential influence on its proneness to fracture. Compared to defect-free pipeline sections, the material will be more actively damaged (also as a result of strain ageing) in the zones of location of the defects characterized by a high stress concentration and dimensions close to the critical values. The influence of such defects, of predominantly technological origin, on pipeline ruptures, is most often manifested in the initial periods (running-in) although the possibility of greater activity of growing defects in later periods of pipeline operation, cannot be eliminated, either.

Further investigations are required in order to more precisely determine the regularities of development of the ageing processes and their influence on damageability of the pipeline materials. This is primarily related to assessment of the factor of long-time force loading as the main kind of impact. The features of ageing of steel strengthened during controlled rolling, should be specially studied. On the other hand, generalization of the available practical data and the current concepts on the nature of steel ageing phenomena, permit making the following statements as regards the processes of pipe metal ageing. The steels for the main pipelines can be regarded as the materials prone to the ageing processes. In principle, the probability of change of the most important service properties of pipe metal should not be denied.

Material ageing proper, especially at its initial stage, does not in any way eliminate the possibility of their further use. It should be noted that the data on the level of the residual service properties which the material has and which determine the further operability of the pipelines, are important for practical work. The pipeline operation parameters should allow for the changes in the material properties as a result of its ageing. As ageing can increase the risk of failure, the temperature and loading modes of aged pipelines operation should be corrected, if required. The sections of conside rable damage of the material, for instance, in the case of intensive corrosion, should certainly be restored.

The problem of time dependence of the change in the level of properties of the material of the actual pipelines and other structures in service still remains to be the most complicated and, unfortunately, unclear issue. The degree of material degradation will indubitably be determined by many circumstances, namely the totality and intensity (aggressiveness) of the acting factors, such as loads, temperature changes, contacting media inside and outside the pipelines; effectiveness of the «protective» measures (electrochemical protection, monitoring and maintenance of the required technical condition of the pipeline) and, furthermore, material ability inherited from the initial condition (including the reliability of passive anticorrosion protection) to resist service impacts or the so-called spontaneous changes running in time, and related to the increase of entropy. The regularities of the change of the pipeline material service properties in time established in a number of studies, are far from being universal. They characterize the changes which occurred in the condition of materials of specific pipelines. For the actual practical operation of the main pipelines, something else is not less important, in principle. It is quite possible that

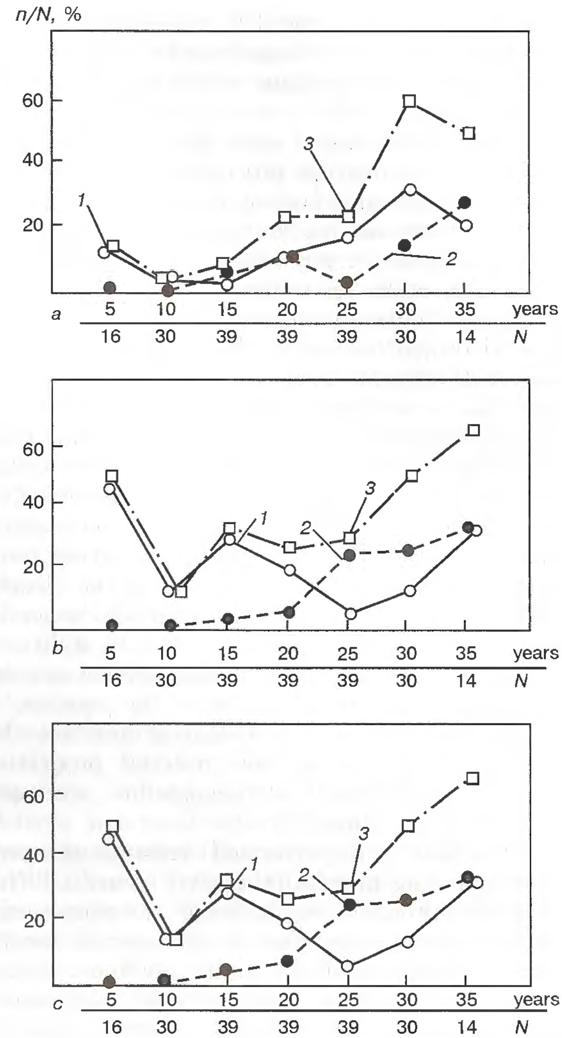

Pipeline failures depending on their period of operation: *a* – *c* — nominal diameter of 500; 700 and 800; 1000 and 1200 mm, respectively; *1* — defects of the metal (pipe butt); *2* — corrosion; *3* — total failures

in many cases the duration of the stage characterized by comparatively slight changes of the structural state and service properties of the metal[*], will be commensurate with the planned pipeline operational periods.

The factor of metal ageing, in terms of the associated adverse consequences such as ductility drop, embrittlement, fracture, will obviously be manifested under the conditions of highly intensive impacts. The risk of pipeline failure as a result of material ageing, arises if no effective measures are taken during the pipeline operation in order to prevent the increase of the working pressures above

* Apparently, it will be necessary to more precisely define the terminology for a more accurate and definite interpretation of the essence of the phenomena and the main causes leading to metal ageing. In our opinion, for instance, the term «long-term strength (static, cyclic)» is preferable to the material «ageing» term in evaluation of the influence of long-term loading at a standard level.

the specified values, metal hydrogenation, intensive cyclic loads; detect and eliminate the deviations from pipeline position or sections of pipeline damage.

Ageing of the metal subjected to cold plastic deformation during pipe processing, if it is limited to the standard value (not more than 1.2 % in pipe expansion) does not lead to formation of hazardous structural states or any essential changes of the service properties, respectively.

The most noticeable changes of the physico-mechanical properties responsible for fracture resistance, will proceed in the local zones of concentration of plastic deformations which accumulate during technological processing and operation (defects, local distortions of the shape in base metal and especially in the welded joints). The intensive plastic deformations developing in the overstressed zones because of land sliding, support shifting, temperature and other impacts leading to the change of the pipeline position, can also lower the metal ductility and toughness margin and, in addition, increase its susceptibility to embrittlement as a result of ageing in further service of the pipeline.

Thus, local or localized damage and not the overall deterioration of the material properties along the entire length of the pipeline, are more probable in operation.

The results of the performed investigations provide convincing proof of the need to use a differentiated approach to evaluation of the phenomena of metal ageing, depending on the specific conditions of operation of the main pipelines, initial quality characteristics of the material, aggressiveness of the contacting media, etc., which predetermines the actual kinetics of the possible changes in the material conditions.

The methodology of evaluation of the condition of the operating pipelines or pipelines whose specified life is over, should provide the possibility of detection of the residual service properties and parameters which characterize the material performance margin or residual performance. Such an approach is precisely defined in [11], and it implies performance of a series of investigations including destructive testing of material samples for evaluation of the actual margin of its strength and crack resistance. A similar approach is also formulated in other publications on the condition of materials of operating pipelines as the fatigue life of the above constructions is determined exactly by the service properties margin.

It should be noted that evaluation of the residual service properties of the material gives an idea about the condition of the object as a whole, including the probable local damage zones. It is evident that with decreased service properties the material proneness to formation of the fracture sites will increase, and, thus appropriate evaluation of the material will indicate the level of risk of its possible damage in service.

Detection of «active» local zones in the pipeline in which material pre-fracture sites are formed, is of importance in itself. Changes in the material condition in the above active zones, are controlled in the most reliable fashion, by the method of acoustic emission [12, 20].

Similar to identification of any other system condition, evaluation of the state of material of an operating main pipeline is based on revealing the parameters which characterize the material and referring it by the set of these parameters to a certain class, type, category, group, etc., according to the classification of material states.

For the case of pipe metal, actually similar to material of other structures, a classification can be proposed which envisages three groups of material conditions at minimum, namely operable condition, limited performance condition, and pre-failure condition. The material condition which provides pipeline operation at the design working load parameters without any limitations should be considered the operable condition. A condition of materials in which in order to achieve the design working load parameters it is necessary to satisfy certain additional conditions (for instance, absence of damage) or take certain measures to restore the material performance, is regarded as the limited performance condition. A pre-failure condition is such a condition of the material in which a considerable risk of failure arises at the design working load parameters due to loss of tightness, or stability of the structure or pipeline rupture.

It is recommended to develop the evaluation criteria and limit values of the parameters for the above material conditions proceeding from the formed approaches to ensuring the structural strength of materials of the pipeline load-carrying elements.

According to [21] the structural strength of the pipe metal is provided by the use of sheet or coiled steel with the required quality indices, guaranteed characteristics of geometrical parameters, continuity and mechanical properties, as well as the specified technologies of pipe fabrication and control. The above approach to provision of the structural strength can be also applied to the material (base metal and welded joints) of the pipelines in service. However, in the case of the operating pipelines, the set of parameters controlled at the stages of pipe fabrication and pipeline construction, should be complemented, allowing for revealing a possible change in the state of materials under service impacts, during the performed repairs, etc.

It is obvious that the finished pipes, including the pipes from the emergency stock of the companies, pipelines approved for service and those currently in operation, whose base metal and welded joints fully meet the requirements of SNiP codes, standards, rules, specifications and other regulatory documents currently in force, should be regarded as serviceable.

For the pipelines currently in service, the parameters which can change under the influence of the service impacts, and, therefore, act as criteria in determination of a certain material condition according to the developed classification, acquire primary importance. Geometrical parameters, mechanical properties, structural characteristics, continuity parameters, physical and other properties can be regarded as such. The analyzed parameters should either directly or indirectly characterize the material capability to stand the specified loads. The parameters which reflect the consequences of service factors impact on the material should be defined, thus permitting material performance to be predicted for a specified range of working loads and service conditions while allowing for the changes which have taken place in the materials.

Thus, the intent is to primarily determine the parameters of the state of the material and, proceeding from the established (or currently developed) methods of analytical assessment, to control the strength margins of various sections of the operating pipelines. It is evident that the above approach does not eliminate the possibility or the need for a special additional evaluation of the criticality of the local damage areas which are becoming active. In view of the diversity of individual features, evaluation of the strength of such pipeline sections requires an independent analysis taking into account the specific circumstances, namely the nature of the stressed-strained state, kind of damage, development of the cracking processes, etc. These issues are not treated in this paper.

Table 2 presents in more detail the characteristics of the proposed classification approach to evaluation of the state of materials of the operating pipelines and also indicates the possible methods of determination of the parameters of the condition of materials of the operating pipelines. The actual inspection procedures are the subject of special development carried out in terms of the scope of technical diagnostics of the pipelines. Useful recommendations in this respect are contained in [11, 12, 14, 20, 22, 23, etc.].

It should be emphasized that considerable attention should be given to mechanical properties which directly characterize the material capability to stand service loads. Unlike the procedure of control in pipe production, when diagnostic of operating pipelines is performed, it is practically impossible to acquire the statistical data on the material mechanical properties after a certain period of operation. Nonetheless, the measures taken during provision of the appropriate technical condition of the pipelines enable selective control of the service properties of the material on the coils cut out of the pipeline. Considering the difficulties of forecasting the kinetics of the processes of material ageing under service impacts, the diagnostic units of the companies or appropriate centers should not neglect such possibilities. It is necessary to develop coordinated criteria and methods of NDT of the material mechanical properties with their adaptation to the factory and route conditions.

The proposed classification clearly defines the practical orientation of the activities of the companies operating the line pipelines. The most complicated task certainly is determination of the parameters of further operation of the pipelines whose material is in the limited performance condition. Similar to what was noted for the metal ageing phenomena, the limited performance condition does not eliminate the possibility of further operation of the pipelines. However, the loading, temperature and other working modes of such pipeline operation should be corrected, if required, allowing for the changes which have taken place in the materials.

With a considerable scope of production and application of the pipe products, especially in the previous years, when the used technologies and methods of material control were less perfect, there is a possibility of revealing in diagnostic inspection of the pipelines, individual pipes (or welded joints) with defects, structural imperfections or other deviations from the standard characteristics, present in the materials already in their initial condition. In terms of classification of the condition of the material of the operating pipelines, the presence of such deviations is a factor of limitation of the material performance. Nonetheless, in individual cases, a decision can be taken on preservation of the same working parameters of further loading of the pipeline. In this connection, it is rational to introduce additional gradation of the degree of material damage in operation. In Table 2 the area of limited performance is crossed by a conditional boundary line which separates the condition of slight, «uniform» structural damage from the condition characterized by more hazardous irreversible damage of the metal which precedes crack initiation. In the latter case, certainly, more effective measures should be taken to provide a reliable performance of the pipeline. Some other important circumstances should also be noted. The set of standard requirements to the initial pipe material does not completely take into account the possible influence of service impact. Certain attempts to improve the situation have been made in [21], however, the recommendations elaborated in this document, are not yet fully taken into account in practice.

As regards pipe steels, especially the initial condition of the materials, there is a lack or an extremely limited amount of certain required basic information which would permit evaluation of the changes in the pipe metal after certain period of operation. There is an obvious need for accumulation of the appropriate data also for currently produced pipe steels. Determination of the level of mechanical properties of the initial pipe material with application of non-destructive methods, which are of interest for evaluation of the material condition in pipeline operation, acquires special importance as was already noted. It is also rational to elaborate new approaches to design of the pipeline systems taking into account monitoring of the technical condition of the material in the characteristic sections of the route [12].

CONCLUSIONS

1. Proceeding from the performed investigations, it can be assumed that in many cases the material of the pipeline load-carrying elements (base metal and welded joints) will preserve a high performance after long operational periods and, therefore, will be able to ensure further safe operation of the pipelines.

2. The most noticeable changes of the physico-mechanical properties of the material under the influence of the service impacts can take place in local sections with defects, stress raisers, deformed zones and various damage. Detection and elimination of the above hazardous zones is a priority task for provision of long-term, safe and reliable operation of the main pipelines.

3. The hazard of pipe metal embrittlement becomes greater, if no effective measures are taken to prevent plastic deformation, intensive cyclic loading, metal hydrogenation, detect and repair the damage in time. In connection with a higher susceptibility to ageing, it is also necessary to take measures for limiting the work hardening of the metal of the local zones under technological impact, including pipe billet expansion.

4. In view of the diversity of the influencing factors and the difficulties of forecasting the consequences of the ageing processes in evaluation of the technical condition of the materials of the operating pipelines, a differentiated approach should be used, allowing for the features of the specific types of materials, loads and external impacts. A most important goal in examination of pipelines operating for a long time is determination of the residual service properties and structural state of the pipe metal. The proposed in this paper approach to classification of the material conditions will permit this problem to be solved in a more reliable manner in the actual practice of examination of the operating pipelines.

5. The accumulated experience in the field of the operating pipelines examination is insufficiently taken into account in development of the standards for pipe products. It is rational to expand the range of the controlled parameters of pipe metal, which will later on permit tracing the possible changes in its condition more accurately during long term service.

REFERENCES

1. Ivantsov, O.M. (1989) Reliability and ecological safety of the main pipelines of Russia. In.: *Transact. of the Int. Conf.*, Kyiv, Nov. 1998. Kyiv: PWI.
2. Steklov, O.I. (1989) Monitoring and forecasting the life of welded structures allowing for their ageing and corrosion. *Ibid*.
3. Gumerov, A.G., Zainulin, R.S., Yamaleev, K.N. *et al.* (1995) *Ageing of oil pipelines*. Moscow: Nedra.
4. Steklov, O.I. (1998) Monitoring and assessment of the predicted life of oil and gas facilities. *Ekologia Okruzh. Sredy i Zashchita ot Korrozii*, **1**, 2 – 8.
5. Goritsky, V.N. (1998) Non-destructive method of diagnostic of embrittlement and change of crack resistance characteristics. *Ibid.*, 15 – 19.
6. Chaburkin, V.F. (1998) Formation of sites of gas and oil pipeline failures under the conditions of actual loading. *Ibid.*, 20 – 23.
7. Kuznetsov, V.V. (1997) Brief analysis of failures of large-diameter pipelines. In: *Transact. of Conf. on Improvement of the Operational Reliability of Large-diameter Pipes of the Main Pipelines.* Volzhsky.
8. Sergeeva, T.K., Volgina, N.I., Ilyukhina, M.V. *et al.* (1993) Corrosion cracking of gas pipeline pipes in low-acid soil. *Gaz. Promyshlennost,* **7**, 34 – 35.
9. Mazel, A.G. (1993) On stress corrosion of gas pipelines. *Ibid.*, 36 – 39.
10. Marchenko, A.F. (1995) Soil corrosion of pipeline steel and the main pipelines. *Stroitelstvo Truboprovodov,* **1**, 29 – 34.
11. Pashkov, Yu.I., Anisimov, Yu.I., Lanchakov, G.A. *et al.* (1995) Forecasting the residual strength margin of the main gas and oil pipelines allowing for the period of operation. *Ibid.*, 2 – 5.
12. Paton, B.E., Nedoseka, A.Ya. (1998) On provision of safe service of welded structures and constructions. *Avtomaticheskaya Svarka*, **11**, 20 – 25.
13. Lanchakov, G.A., Stepanenko, A.I., Pashkov, Yu.I. (1994) Influence of the time of operation on the pipeline strength margin. *Gaz. Promyshlennost,* **3**, 11 – 12.
14. Grudnisty, V.I., Zorin, E.E., Egurtsov, S.A. *et al.* (1996) *Repair of the main and production gas pipelines*. Kyiv: Intergrafic.
15. Ivanstov, O.M., Kharitonov, V.I. (1978) *Reliability of the main pipelines*. Moscow: Nedra.
16. Paton, B.E., Medovar, B.I., Semenov, S.E. *et al.* (1999) Pure pipe metal: achievements, prospects, problems. *Problemy Spets. Electrometallurgii*, **2**, 9 – 26.
17. Mochernyuk, N.P., Krasnevsky, S.M., Lazarevich, G.I. *et al.* (1991) Influence of the length of operation of the main gas pipelines and working pressure of gas on the physico-mechanical characteristics of 19G pipe steel. *Ibid.*, **3**, 34 – 35.
18. Khorionovsky, V.V. (1994) Problem of service life of gas pipeline structures. *Ibid.*, **7**, 17 – 20.
19. Tarlinsky, V.D., Golovin, S.V. (1997) Experimental evaluation of the properties of the metal of gas pipelines operating for a long time. *Stroitelstvo Truboprovodov,* **1**, 29 – 32.
20. Nedoseka, A.Ya. (1998) *Fundamentals of design and diagnostic of welded structures*. Kyiv: INDPROM.
21. (1998) *SP 34-101–98. Selection of pipes for the main oil pipelines in construction and overhauling*. Moscow: Transneft.
22. Kharionovsky, V.V. (1995) Diagnostic and life of pipelines: status and prospects. *Gaz. Promyshlennost,* **11**, 28 – 30.
23. Chernyaev, V.D., Chernyaev, K.V. (1998) Provision of safe service and extension of service life of the main oil pipelines based on wide-scale diagnostic activities and effective repair techniques. In: *Proc. of 4th Int. Conf.-exhib. on Problems of Corrosion and Anticorrosion Protection of Materials,* Lvov, June 9 – 11, 1998.

Table 2. Proposals on evaluation of the state of material (base metal and welded joints) of pipelines in operation

<table>
<tr><th rowspan="3">Criteria of material state evaluation</th><th rowspan="3">Material state parameters</th><th colspan="4">Approaches to determination of the limit (threshold) values of the parameters for different degree of damage and different conditions of the material</th><th rowspan="3">Methods of investigation</th></tr>
<tr><th colspan="2">Minor (slight) damage</th><th colspan="2">Pronounced (strong) damage</th></tr>
<tr><th>Operable condition</th><th colspan="2">Limited performance condition</th><th>Prefailure condition</th></tr>
<tr><td rowspan="9">Structural shape and fabrication technology</td><td rowspan="9">Diameter, wall thickness, ovality and other deviations from the shape. Displacement and angularity of edges mating and sequence of weld performance, etc.</td><td rowspan="9">In keeping with the requirements of SNiP, rules and other standards currently in force</td><td colspan="3">In case of deviations from the current requirements</td><td rowspan="9">Profilometry and thickness measurement, size measurement (after pitting). Magnetic noise, holography methods, calculation methods, etc.</td></tr>
<tr><td colspan="3">Increase of the perimeter, %</td></tr>
<tr><td>up to 1</td><td>up to 3</td><td>up to 3 and greater</td></tr>
<tr><td colspan="3">Increase of working stresses in the places of wall thickness reduction or deviation of shape (compared to the standard yield point of the steel)</td></tr>
<tr><td>not more than 1.0</td><td colspan="2">1.0 and more</td></tr>
<tr><td colspan="3">Depth of dents (in % of nominal diameter)</td></tr>
<tr><td colspan="2">up to 3.5</td><td>more than 3.5</td></tr>
<tr><td colspan="3">Corrugations, bends («folds»)</td></tr>
<tr><td colspan="2">absent</td><td>present</td></tr>
<tr><td>Composition</td><td>Base alloying and content of impurities</td><td>In keeping with the standard requirements</td><td colspan="2">Deviation from standard in composition</td><td>Does not correspond to the specified steel grade (lower strength category), higher content of hydrogen</td><td>Analysis of the pipe material composition determined on samples cut out of a pipeline. Metal control at the increase of the pipe perimeter is required</td></tr>
<tr><td rowspan="7">Mechanical properties</td><td>Standard characteristics (σ_y, σ_t, δ_5, ψ, bend angle, KCV, KCU)</td><td>The same</td><td colspan="2">Deviation of individual characteristics of the mechanical properties compared to the standard characteristics</td><td>$\sigma_y/\sigma_t \to 1$ or low values of mechanical properties because of cracks (microcracks) or intergranular fracture</td><td rowspan="8">Breaking tests of the material when studying representative samples cut out of the pipeline. Preliminary evaluation is possible by the results of measurement of the hardness and magnetic properties of the material</td></tr>
<tr><td rowspan="2">Temperature of transition into the brittle state T_b (DWTT, Charpy type samples)</td><td>$T_b \leq T_r$</td><td colspan="3">$T_b > T_r$</td></tr>
<tr><td colspan="4">T_r is the minimal rated temperature of pipeline operation</td></tr>
<tr><td rowspan="4">Crack resistance at temperature T_r (standard and other rated values)</td><td colspan="4">Cracking indices (compared to similar values for the initial condition of the material)</td></tr>
<tr><td>comparable</td><td colspan="2">lower</td><td>low</td></tr>
<tr><td colspan="4">Fracture mode</td></tr>
<tr><td colspan="2">tough</td><td colspan="2">quasibrittle</td></tr>
<tr><td rowspan="2">Structural state</td><td rowspan="2">Microstructure (grain size, segregation, contamination with non-metallic inclusions, hardness, etc.)</td><td rowspan="2">In keeping with standard recommendations. Characteristic of this type of steel and welded joint</td><td colspan="3">Deviation from the recommended values and lack of the structural parameters correspondence to this type of steel and welded joint</td></tr>
<tr><td colspan="2"></td><td>Cracks in the metal, zones of quenching structures with more than HV 350 hardness</td><td>Microstructural and fractographic investigations of samples</td></tr>
</table>

Table 2 (cont.)

<table>
<tr><th rowspan="3">Criteria of material state evaluation</th><th rowspan="3">Material state parameters</th><th colspan="4">Approaches to determination of the limit (threshold) values of the parameters for different degree of damage and different conditions of the material</th><th rowspan="3">Methods of investigation</th></tr>
<tr><th colspan="2">Minor (slight) damage</th><th colspan="2">Pronounced (strong) damage</th></tr>
<tr><th>Operable condition</th><th colspan="2">Limited performance condition</th><th>Prefailure condition</th></tr>
<tr><td></td><td>Substructure (dislocation density, microstress gradients, heterogeneity of interfacial junctions, etc.)</td><td colspan="2">Different stages of a uniform subgranular structure formation</td><td colspan="2">Pronounced interphase and intergranular heterogeneity, formation of phase precipitations which promote the increase and concentration of microstresses, microstrain accumulation, etc.</td><td></td></tr>
<tr><td rowspan="20">Defects and damage</td><td>Delaminations, process defects of welding</td><td>In keeping with the standard requirements</td><td colspan="3">Exceeding the standard requirements in size and number. Coming to the weld boundary</td><td>Thickness measurement</td></tr>
<tr><td rowspan="4">Cracks</td><td colspan="4">Cracks of various origin oriented across or at an angle to the surface, including those propagating in the zones of location of the initial defects and stress raisers</td><td rowspan="4">Visual examination and NDT (UT, AE, etc.) of the pipeline section</td></tr>
<tr><td colspan="2" rowspan="3">absent</td><td colspan="2">present</td></tr>
<tr><td colspan="2">Crack size</td></tr>
<tr><td>subcritical</td><td>close to critical</td></tr>
<tr><td rowspan="7">Surface damage (mechanical, corrosion-abrasive wear, etc.)</td><td rowspan="7">Shallow damage not reducing the wall thickness below the admissible limits (general and pitting corrosion, traces of abrasive wear, small scratches, marks, etc.)</td><td colspan="3">Damage of different origin reducing the wall thickness below the admissible limit</td><td rowspan="7">Determination of «dangerous» zones during corrosion examinations. Microstructural investigations. Design methods of evaluation of the strength of defective sections of pipelines</td></tr>
<tr><td colspan="3">Increase of working stresses in the points of defect location (in relation to the standard yield point of steel)</td></tr>
<tr><td>up to 0.9</td><td>up to 1.0</td><td>1.0 and more</td></tr>
<tr><td colspan="2" rowspan="4"></td><td>Mechanical damage in the dent zone</td></tr>
<tr><td>Burrs, nicks along the weld fusion line</td></tr>
<tr><td>Length of crack-like defects comparable with the critical size of the crack</td></tr>
<tr><td>Local kinds of corrosion at the damage depth equal to 0.5 of the wall thickness and more</td></tr>
<tr><td rowspan="6">Accumulation of microdefects and damage propagation</td><td colspan="4">AE activity characterizing the susceptibility to crack initiation and propagation</td><td rowspan="6">Breaking tests with simultaneous AE-monitoring. AE-monitoring in site</td></tr>
<tr><td colspan="2">weak</td><td>increased</td><td>high</td></tr>
<tr><td colspan="4">Continuous AE component</td></tr>
<tr><td>absent</td><td colspan="3">present</td></tr>
<tr><td colspan="4">Discrete AE component</td></tr>
<tr><td colspan="3">absent</td><td>present</td></tr>
<tr><td rowspan="2">Corrosion properties</td><td rowspan="2">Corrosion intensity</td><td colspan="4">Corrosion rate (compared to respective value for the material initial condition)</td><td rowspan="2">Chemical methods of investigations when using model aggressive media. Pipeline examination for corrosion damage</td></tr>
<tr><td colspan="2">comparable</td><td colspan="2">increased</td></tr>
</table>

MATHEMATICAL MODELLING OF ABSORPTION OF GASES BY METAL DURING WELDING

I.K. POKHODNYA, V.I. SHVACHKO and **O.M. PORTNOV**
The E.O. Paton Electric Welding Institute, NASU, Kyiv, Ukraine

ABSTRACT

Results of mathematical modelling of absorption of hydrogen and nitrogen by iron during welding are presented. The kinetic model of interaction of the low-temperature plasma with metal, based on the combined solution of equations of mass transfer in gas and metal, has been developed. Comparison of calculation results and experimental data shows that the model developed adequately describes absorption of two-atomic gases by metal. The process of absorption of gases by the molten metal pool from the low-temperature plasma has been calculated. The above model allowed the effect of the plasma temperature on the concentration of gas dissolved in metal to be estimated.

Key words: *mathematical modelling, low-temperature plasma, absorption of hydrogen and nitrogen, equation of mass transfer, Boltzmann equation.*

Gases dissolved in metal exert a considerable effect on mechanical properties of a welded joint. Nitrogen causes an increase in yield and tensile strength and a decrease in ductility. Hydrogen initiates cold cracking [1]. To predict the content of gases in the weld, it is necessary to understand the mechanism of their dissolution in metal. Direct measurements of absorption of gases by metal during the welding process involve difficulties, whereas mathematical modelling provides additional information on the process of absorption of gases by metal.

Transfer of the impurity elements in the metal–gas system is determined from a system of equations that describe gas-dynamic motion of particles in the plasma, molecular interaction in the Knudsen subsurface layer and redistribution of an impurity in the welded joint metal. Description of the gas-dynamic motion near the surface of a solid body is based on the kinetic theory of gases [2].

Physical model of absorption of gases. Absorption of gases by metal consists of several stages [3]: motion of the gas molecules to the surface, dissociation of molecules on the surfase, adsorption of atoms by the metal surface and diffusion of atoms into the bulk of metal or melt. Absorption is usually accompanied by desorption of gases. To describe distribution of gas in metal it is necessary to determine the total gas flow over the metal–gas interface at each time moment during the entire process. The total gas flow to the metal is equal to difference between the direct (absorption) and reverse (desorption) flows. The direct flow is determined by the state of the metal surface and ambient atmosphere, while the reverse flow depends mostly upon the state of the metal surface, i.e. its temperature and dissolved gas content of the metal interface. It should be noted that not all collisions of the gas molecules with the metal surface are accompanied by chemical reactions (dissolution or formation of a chemical compound). Molecules reflected from the surface interact with both direct and reverse gas flows.

Gases are dissolved in metal in the atomic state, and the rate of absorption of multi-atomic gases from the atmosphere depends upon the degree of dissociation of the molecules, which occurs both on the heated metal surface and directly in the bulk of a gas. Therefore, the physical model of absorption of gases is constructed with allowance for the following assumptions:

gases are dissolved in metal only in the atomic state;

every gas atom, upon collision with the metal surface, penetrates into the bulk of the metal;

non-dissociated molecules are diffusely reflected from the metal surface;

at the absence of the plasma, dissociation of the gas molecules occurs at the heated metal surface;

dissociation of the gas molecules in the plasma occurs directly in the bulk of the metal;

intensity of desorption of gas from the metal depends upon the surface temperature and surface concentration of the dissolved gas atoms;

no convective stirring of the metal occurs, the gas atoms in the metal move by the diffusion mechanism;

pressure of the plasma in the discharge gap is equal to the atmospheric pressure at a substantial distance from the arc discharge region.

Basic physical processes occurring near the metal–gas interface, i.e. at a molecular level in interaction of metal with the low-temperature plasma, are schematically shown in Figure 1. The diagram of a space structure of the problem of mass transfer and the selected system of coordinates are shown in Figure 2.

© I.K. POKHODNYA, V.I. SHVACHKO and O.M. PORTNOV, 2000

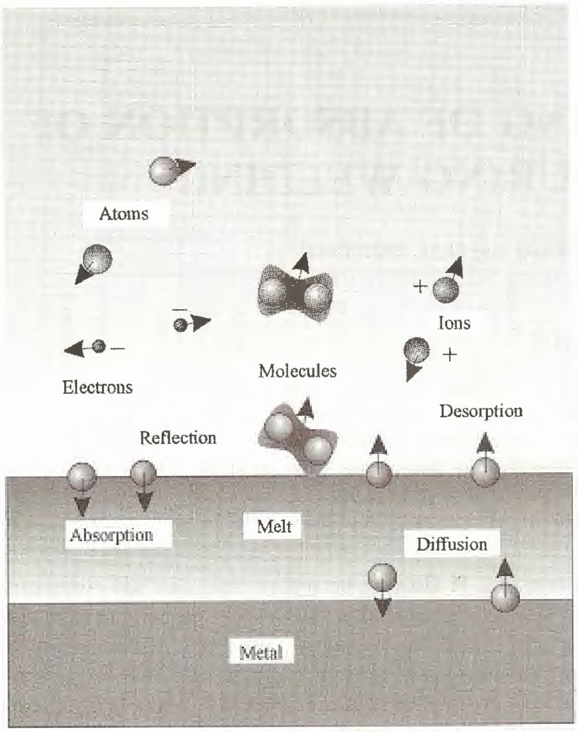

Figure 1. Schematic of the basic molecular processes occurring in the Knudsen layer in interaction of plasma with metal

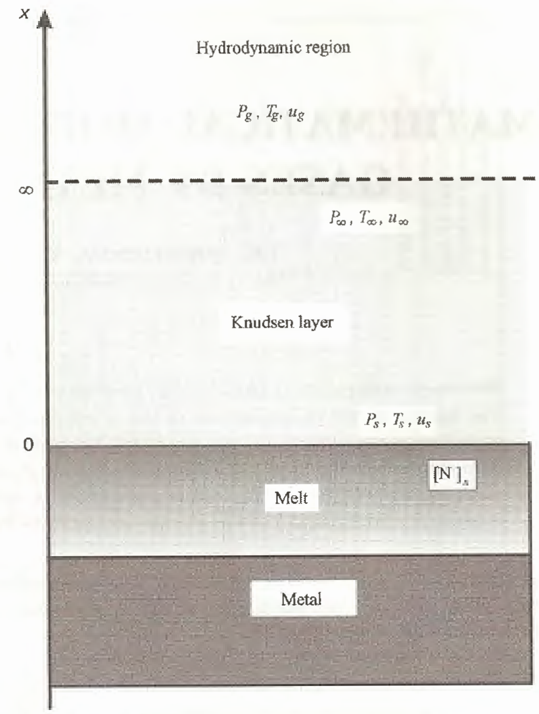

Figure 2. Diagram of the space structure of the gas flow in its interaction with metal

Mathematical model. The mathematical model of absorption of gases, taking into account basic physical processes occurring in dissolution of gases, as well as geometrical structure of the problem, was constructed as follows.

Given that there is no convective stirring, that the depth of distribution of an impurity in the metal is smaller than transverse sizes of the HAZ and the radius of curvature of the metal surface is much larger than the free path of particles in gas, the problem may be considered in a unidimensional statement. In this case the impurity distribution in the metal by a diffusion mechanism can be described by the following equation:

$$\frac{\partial C}{\partial t} = \frac{\partial}{\partial x}\left(D\,(T)\,\frac{\partial C}{\partial x}\right). \qquad (1)$$

The initial ($t = 0$) and boundary ($x = 0$, $x = -\infty$) conditions for equation (1) have the following form:

$$C\,(x,\,0) = C_0,\;\; C\,(-\infty,\,t) = C_0,$$
$$-D\,(T)\,\partial C/\partial x|_{x=0} = j,\;\; D\,(T)\,\partial C/\partial x|_{x=-\infty} = 0.$$

The following designations are used in equation (1): $C = C\,(x,\,t)$ is the concentration of the impurity element; D is the diffusion coefficient; $T = T\,(x,\,t)$ is the metal temperature; x is the space coordinate directed from the metal to the gas phase and t is the time. The gas content of the metal, [G] (wt.%), depends upon concentration C as follows: $[G] = (C/\rho)\cdot 100$ %, where ρ is the specific metal density.

Dependence of the diffusion coefficient of gases in molten iron upon the temperature is described by the following law: $D = D_0 \exp(-T_D/T)$. Values of constants D_0 and T_D for nitrogen and hydrogen in iron are given in [4].

Density of the total mass flow of gas into the melt, j, included into diffusion equation (1) as the boundary condition, is associated with the function of distribution of the gas molecules depending upon the velocities in the following way:

$$j = -\int m\, v_x\, f\, d\,\mathbf{v}, \qquad (2)$$

where $\mathbf{v}$ is the vector of the velocity of the gas molecules with components (v_x, v_y, v_z); m is the mass of a gas molecule and f is the function of distribution of the gas molecules depending upon the velocities.

The distribution function $f\,(x,\,\mathbf{v})$ is determined from solution of the gas-kinetic equation for the Knudsen layer adjoining the metal surface. The method of solution described in [5, 6] is based on a bimodal approximation of the distribution function $f\,(x,\,\mathbf{v})$ by the sum of products of the unknown coefficients $a_i^{\pm}(x)$, which are the function of space coordinate x and depend only upon the velocity of the half-space maxwellians $f_i^{\pm}(\mathbf{v})$. In a general form, the half-space maxwellians are described as follows:

$$f_i^{\pm}(\mathbf{v}) = n_i\left(\frac{m}{2\pi k T_i}\right)^{3/2} \exp\left[-\frac{m((v_x - u_i)^2 + v_y^2 + v_z^2)}{2kT_i}\right]. \qquad (3)$$

Sign ± in equation (3) corresponds to a direction of the velocity of motion of the molecules in the gas phase: + — for the molecules which move from the surface and − — for the molecules which move to the metal. Subscript i runs the s, $*$, and ∞ values. Here symbol s designates parameters of the distribution function near the metal surface and symbol ∞ designates parameters of the distribution function at the external boundary of the Knudsen layer. Symbol $*$ designates the gas molecules which left metal but came back to the metal surface as a result of collisions between each other. Parameters n_i, T_i and u_i designate density, temperature and velocity of the mass flow of the molecules, respectively. The unknown functions $a_i^{\pm}(x)$ at the external boundary of the Knudsen layer ($x = \infty$) satisfy conditions $a_s^{\pm} = 0$, $a_*^- = 0$, $a_\infty^+ = 1$, $a_\infty^- = 1$. Therefore, parameters n_∞, T_∞ and u_∞ correspond to a macroscopic density, temperature and mass flow of gas between the Knudsen layer and the gas-dynamic region. The values of coefficients $a_\infty^+ = 0$ and a_s^+ at the metal surface ($x = 0$) are determined from a condition according to which the gas molecule, after collision with the surface, either dissociates and penetrates into the metal or is diffusely reflected from it. The values of parameters $u_s = 0$, $u_* = (2kT_s/\pi m)^{1/2}$, $n_* = n_s/2$ and $T_* = (1 - 2/3\pi)T_s$ are determined from conditions of conservation of mass, momentum and energy for the flow of the gas atoms evolved from the metal. In a general form, the distribution function can be written as follows:

$$f(x, \mathbf{v}) = a_s^+(x)f_s^+(\mathbf{v}) + a_*^-(x)f_*^-(\mathbf{v}) + a_\infty^+(x)f_\infty^+(\mathbf{v}) + a_\infty^-(x)f_\infty^-(\mathbf{v}). \quad (4)$$

Unknown coefficients $a_i^{\pm}(x)$, which are part of the distribution function, can be determined by substitution of molecular characteristics $Q_L = m$, mv, $mv^2/2$ (mass, momentum and energy of an individual molecule) into the gas-kinetic equation

$$\int Q_L \mathbf{v} \frac{\partial f}{\partial x} d\mathbf{v} = \Delta(Q_L). \quad (5)$$

For molecular characteristics m, mv, $mv^2/2$ the integral of collisions is $\Delta(Q_L) = 0$, because of the laws of conservation of mass, momentum and energy. Substitution of equation (4) to the system of momentum equations (5) followed by integration allows parameters of the gas flow near the metal surface ($x = 0$) to be related to those at the external boundary of the Knudsen layer ($x = \infty$). The resulting system of equations has the following form:

$$\frac{1}{2}\pi^{-1/2} t_s^{-1/2} p_s + \frac{1}{2}\alpha t_*^{1/2} F_* a_s^-(0) + \frac{1}{2}\alpha F_\infty a_\infty^-(0) = S_\infty, \quad (6)$$

$$\frac{1}{4}p_s + \frac{1}{4}[2tG_* - (1-\alpha)\pi^{1/2}t_s^{1/2}t_*^{1/2} F_*]a_s^-(0) + \frac{1}{4}[2G_\infty - (1-\alpha)\pi^{1/2}t_s^{1/2}F_\infty]a_\infty^-(0) = S_\infty^2 + 1/2, \quad (7)$$

$$\pi^{-1/2}t_s^{1/2}p_s + [t_*^{1/2} H_* - (1-\alpha)t_s t_*^{1/2} F_*]a_s^-(0) + [H_\infty - (1-\alpha)t_s F_\infty]a_\infty^-(0) = S_\infty(S_\infty^2 + 5/2), \quad (8)$$

where

$$a_s^- = a_*^- n_*/n_\infty, \quad t_i = T_i/T_\infty, \quad p_s = P_s/P_\infty,$$
$$S_i = u_i/(2kT_i/m)^{1/2},$$

$$P_i = n_i kT_i, \quad F_i = S_i \operatorname{erfc} S_i - \pi^{-1/2}\exp(-S_i^2),$$

$$G_i = (S_i^2 + 1/2)\operatorname{erfc} S_i - \pi^{-1/2}S_i\exp(-S_i^2),$$

$$H_i = \frac{1}{2}S_i(S_i^2 + 5/2)\operatorname{erfc} S_i - \pi^{1/2}(1 + \frac{1}{2}S_i^2)\exp(-S_i^2).$$

Equations (6) through (8) contain three unknown values: $a_s^-(0)$, $a_\infty^-(0)$ and S_∞. The desired mass flow of gas to the metal is determined through variable S_∞ as follows:

$$j = -\int m\mathbf{v}_x f d\mathbf{v} \equiv -mn_\infty(2kT_\infty/m)^{1/2}S_\infty.$$

The system of equations (6) through (8) includes parameters relating to the boundary of the Knudsen layer and in the ambient atmosphere. Temperature and pressure of the gas phase at the boundary of the Knudsen layer (subscript ∞) and in the region of the hydrodynamic gas flow (subscript g), according to [7], are related by the following equations:

$$T_g/T_\infty = (P_g/P_\infty)^{(\gamma-1)/\gamma},$$
$$P_g/P_\infty = [1 + \frac{1}{2}(\gamma - 1)M_\infty]^{2\gamma/(\gamma-1)}, \quad (9)$$

where $M_\infty = (2/\gamma)^{1/2}S_\infty$ is the Mach number; $\gamma = c_p/c_v$ is the specific thermal coefficient; T_g and P_g are the temperature and pressure, respectively, of the surrounding gas.

To solve the system of equations (6) through (8), it is necessary to determine one more parameter, namely the dimensionless pressure of gas evolved from the metal, i.e. $p_s = P_s/P_\infty$. Intensity of desorption of gas from the metal ($x = 0$) is determined through its pressure in the Knudsen layer, P_s, which in turn depends only upon the temperature of the surface, T_s, and the concentra-

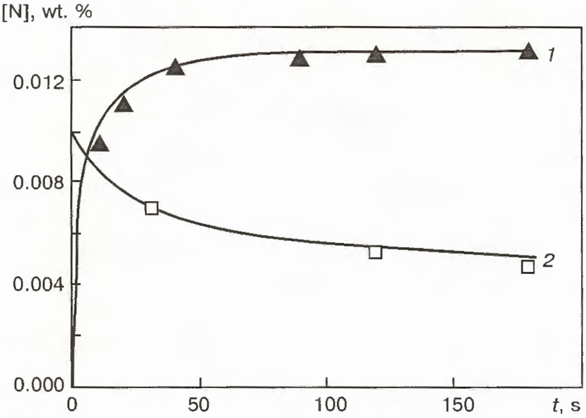

Figure 3. Nitrogen content of iron as function of time of holding a sample in the pure nitrogen atmosphere: *1* — metal remelting; *2* — metal refining; ▲, □ — experimental data obtained at T = 1873 and 1953 K, and P_{N_2} = 0.008 MPa, according to [3]; solid lines — calculation

tion of gas at the surface, $[G]_s$, following the Sieverts law [8], irrespective of the fact whether the metal is in equilibrium with the atmosphere or not. To determine p_s, consider that in a particular case of thermodynamic equilibrium at ($t_s = 1$, $S_\infty =$ $= 0$), as it follows from the system of equations (6) through (8), $p_s = \alpha$. Then

$$P_s = \alpha\,([G]_s/K_G)^2. \qquad (10)$$

Equilibrium constant $K_G = [G]_s/P_s)^{1/2}$ for gas has the following dependence upon the temperature: $\lg K_G = A/T + B$, where A and B are the constants. Their values for nitrogen and hydrogen in iron are given in [3, 9]. In calculations it is important to take into account that dissociation of the gas molecules in the case of contact of the metal surface with a conventional atmosphere occurs mostly at the metal surface as a result of weakening of chemical bond between atoms in the gas molecules near a metal atom [8]. The molecule binding energy E_{d_s} decreases by a value of bond between the atom and metal, E_{M-G}. The degree of dissociation of the molecule near the metal surface is de-

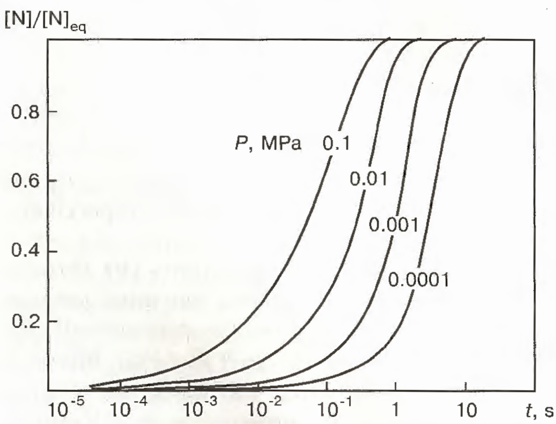

Figure 4. Nitrogen content of iron at a depth of 10 μm as function of time, depending upon the gas pressure at temperature (T = 2000 K)

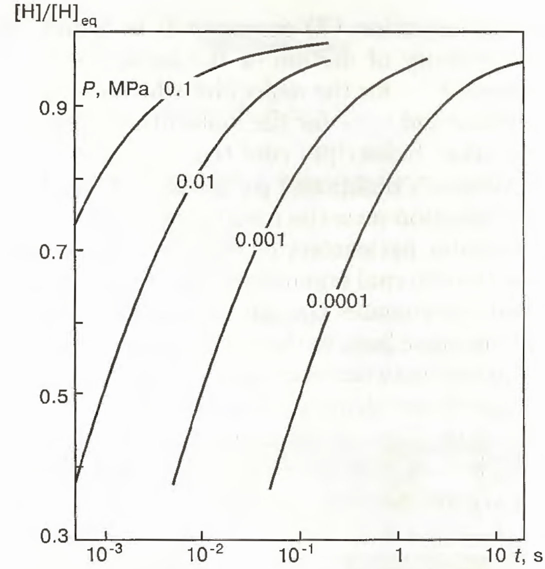

Figure 5. Same as in Figure 4, but for hydrogen

scribed by the Arrhenius law $\alpha = \alpha_0 \exp(-E_d^*/T_s)$, where $E_d^* = E_d - E_{M-G}$. In the case where the metal is in contact with the low-temperature slightly ionized plasma, the molecules dissociate in the bulk of the gas phase (plasma), which is determined by the temperature and density of the latter. Data on the degree of dissociation, depending upon the temperature of the plasma, under a pressure of 10^5 Pa are given below, respectively,

for the nitrogen plasma [10]:

temperature, K	5000	6000	7000	8000
degree of dissociation, α_v	0.20	0.11	0.53	0.91

and for the hydrogen plasma [10]:

temperature, K	4000	5000	6000
degree of dissociation, α_v	0.11	0.45	0.89

The mathematical model was realized in the form of software written in the C++ language. The algorithm of solution of equations of mass transfer is based on the functionally independent modules. The diffusion equation was solved by the finite difference method with approximation of the second order of accuracy, which is provided by the symmetrical implicit «Krank-Nicholson» diagram [11]. The system of non-linear equations (6) through (8) was solved by the tangent method, i.e. the «Newton method», which provides quadratic convergence of the solution [12].

Results and discussion. The process of absorption of gases depending upon the state of the atmosphere can occur under conditions which are both close to thermodynamic equilibrium and far from it, where, for example, the ambient atmosphere is overheated by the electric current flowing through it and, hence, is dissociated to a substantial degree.

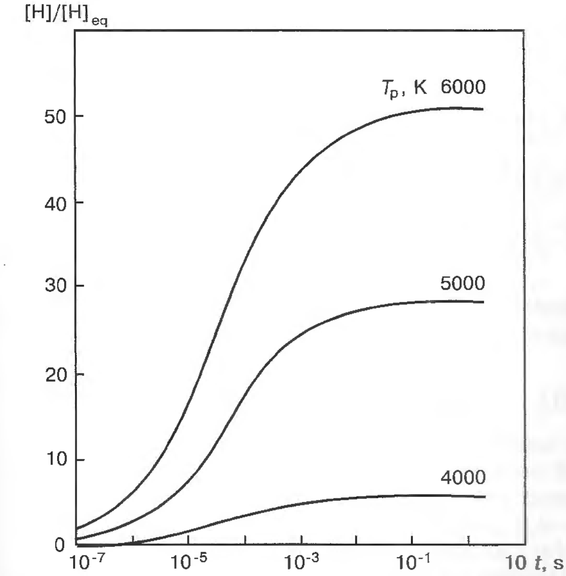

Figure 6. Hydrogen content of iron at a depth of 10 μm as function of time at different temperature of the plasma. Metal temperature 2000 K, partial pressure of hydrogen in the plasma 50 MPa

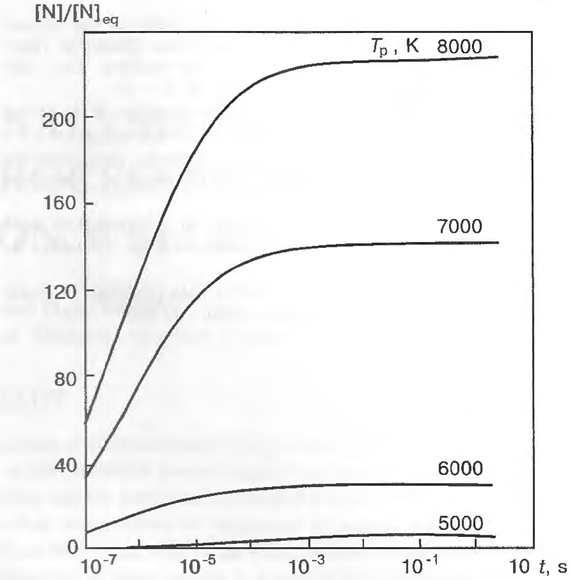

Figure 7. Same as in Figure 6, but for nitrogen. Metal temperature 2000 K, partial pressure of nitrogen in the plasma 500 MPa

The simplest case of mass transfer in terms of investigation is that occurring through the metal–gas interface under conditions close to thermodynamic equilibrium, where the uniformly heated metal is surrounded by gas having the same temperature. Such problems are well studied both theoretically and experimentally. Calculations of the absorption processes under these conditions were used as the test examples to check validity of the developed mathematical model.

Results of the experimental studies of the kinetic dependence of absorption of nitrogen from the controlled atmosphere by the refined metal with an initial nitrogen content of $[N]_0 = 0.001$ %, which are especially convenient for comparing experimental and calculated data, are taken from [3]. Figure 3 shows results of comparison of the experimental and calculated data on the nitrogen content of iron depending upon the time of holding the metal in the atmosphere of pure nitrogen for two different cases: refining and remelting. Note that in the remelted metal the initial nitrogen content $[N]_0$ is lower than the equilibrium concentration $[N]_e$ at a temperature of the melt, whereas metal refining was done at a decreased gas pressure, where $[N]_0 > > [N]_e$.

Calculation of absorption from the pure gas atmosphere depending upon the pressure under conditions of thermodynamic equilibrium is shown in Figures 4 and 5. In calculation of absorption for different gas pressures, the equilibrium gas content calculated following the Sieverts law, $[G] = = K_G P_G^{1/2}$, is taken as the concentration unit. Comparison of Figures 4 and 5 shows that absorption of hydrogen occurs much faster than absorption of nitrogen.

Absorption of gas by metal in contact with the plasma. When the atmosphere transfers into the state of the arc discharge, the degree of dissociation in it increases by many orders of magnitude. Dissociation in the plasma exceeds that of gas on the heated surface, which leads to an increase in the amount of the dissociated atoms in the Knudsen layer. The gas flow into the metal increases and the gas concentration of the metal also substantially increases. Calculation of the kinetic dependence of absorption of gases by the metal in contact with the plasma within the frames of the suggested mathematical model, without description of the dynamics of evolution of the plasma, is presented in Figures 6 and 7. The calculation results make it possible to derive the kinetic dependence of absorption of gases upon the plasma temperature and gas partial pressure and estimate the effect of the plasma temperature on the concentration of gases dissolved in the metal.

CONCLUSIONS

1. The developed kinetic model of interaction of the low-temperature plasma with metal is based on the combined solution of equations of mass transfer.
2. Comparison of the calculation results with the experimental data shows that the developed model adequately describes absorption of two-atomic gases by metal.
3. The model made it possible to estimate the effect of the plasma temperature on the content of gas dissolved in metal.

REFERENCES

1. Pokhodnya, I.K. (1972) *Gases in welds*. Moscow: Mashinostroyeniye.

2. Kogan, M.N., Makashev, N.K. (1971) Role of the Knudsen layer in the theory of heterogeneous chemical reactions and flows with reactions on the surface. *Izv. AN SSSR, Mekhanika zhidkosti i gaza*, **6**, 3 – 11.
3. Averin, V.V., Revyakin, A.V., Fedorchenko, V.I. *et al.* (1976) *Nitrogen in metals*. Moscow: Metallurgia.
4. Linchevsky, B.V. (1986) *Thermodynamics and kinetics of interaction of gases with liquid metals*. Moscow: Metallurgia.
5. Yetrehus, T. (1983) Asymmetries in evaporation and condensation Knudsen layer problem. *Phys. Fluids*, **4**, 939 – 949.
6. Bergstrom, T., Yetrehus, T. (1984) Gas problem in front of a completely absorbing wall. *Ibid.*, **3**, 583 – 588.
7. Velikovich, L., Liberman, M. (1987) *Physics of shock waves in gases and plasma*. Moscow: Nauka.
8. Dembovsky, V. (1981) *Plasma metallurgy*. Moscow: Metallurgia.
9. Morozov, A.N. (1968) *Hydrogen and nitrogen in steel*. Moscow: Metallurgia.
10. Granovsky, V.L. (1971) *Electric current in gases*. Moscow: Nauka.
11. Samarsky, A.A. (1987) *Introduction into numerical methods*. Moscow: Nauka.
12. Molchanov, I.N. (1987) *Mathematical methods for solving of applied problems*. Kyiv: Naukova Dumka.

THERMODYNAMIC ANALYSIS OF REDOX CARBON-INVOLVING PROCESSES OCCURRED DURING FUSION WELDING

N.G. EFIMENKO and **N.A. KALIN**
Ukrainian Engineering-Pedagogical Academy, Kharkov, Ukraine

ABSTRACT

The article suggests an approach to thermodynamic calculation of chemical reactions proceeding in three phases, i. e. metal, slag and gas, at the same temperature. Series of the probable proceeding of reactions of oxidation of elements and reactions of carbon reduction of elements from oxides have been arranged for characteristic temperatures of the melting zone in arc welding. It is shown that temperature of beginning of carbon reduction of oxides in the metal phase, except CeO_2 and FeO, is lower than that in the slag phase which allows the deoxidation process to occur at lower temperatures and provides the possibility of using carbon in a bound state as a deoxidizer in welding consumables.

Key words: *isobar-isothermal potential, chemical affinity, dissociation pressure, phase, oxidation, reduction, oxidizer, reaction constant, melting zone.*

When developing welding consumables for the fusion arc welding an integrated problem of producing gas and slag phases which regulate the weld metal quality during interaction with a metal phase is to be solved. To investigate reactions, proceeding in these phases, from the point of view of the qualitative evaluation and determination of the most probable trend of development, the method is used, as a rule, which is based on setting the thermodynamic equilibrium of the system in the zone of melting.

The comparative estimation of reactions of oxidation is usually carried out by a degree of a chemical affinity of substances to oxygen. The degree of carbon affinity to oxides makes it possible to judge about the process of decarburization in welding.

The measure of a chemical affinity of elements to oxygen in fusion welding serves the increment of a standard isobar-isothermal potential ΔG°_{m}, calculated from Gibbs-Helmholtz equation, which for the preset temperature has a form [1]

$$\Delta G^{\circ}_{T} = \Delta H^{\circ}_{T} - T\Delta S^{\circ}_{T}. \qquad (1)$$

In parallel with an estimation of affinity by decrease in an isobar potential, in thermodynamic analysis of equilibrium of the chemical reaction the calculation of constants of equilibrium, representing the steady relation between the concentrations, participating in the reaction of substances, is used. Dependence of constants of equilibrium on temperature is expressed by the Van't Hoff equation [2]

$$\lg k = -\frac{\Delta G^{\circ}_{T}}{19.15\,T}. \qquad (2)$$

For practical calculations this equation is written in the form

$$\lg k = \frac{A}{T} + B, \qquad (3)$$

where A and B are the constants, whose values are given in reference tables or calculated by known values [2].

The chemical affinity of elements to oxygen is evaluated by the dissociation pressure of oxides and expressed by a partial pressure of the only gaseous product of the reaction, i. e. oxygen.

The work is aimed at the determination of sequence (preference) of proceeding reactions of formation of oxides and carbon reduction of elements from oxides in three phases at the same temperatures.

The thermodynamic analysis was performed using the data of [3, 4] for reactions occurring in fusion welding with an involvement of iron, manganese, titanium, aluminium, carbon, yttrium, zerium and their oxides.

To study the reactions proceeding in a molten metal, a temperature interval of existence of a liquid metal phase (electrode drops, weld pool) was taken, beginning with a minimum possible temperature of Fe–C alloy melting from the equilibrium diagram [5], equal to 1420 K, that corresponds to 4.3 % C-containing eutectics. The temperature of drops of the electrode wire Sv-08, equal to 2500 K, is taken as a maximum temperature of the metal phase, while 1810 K is taken as a temperature of beginning of melting of this electrode rod [6].

© N.G. EFIMENKO and N.A. KALIN, 2000

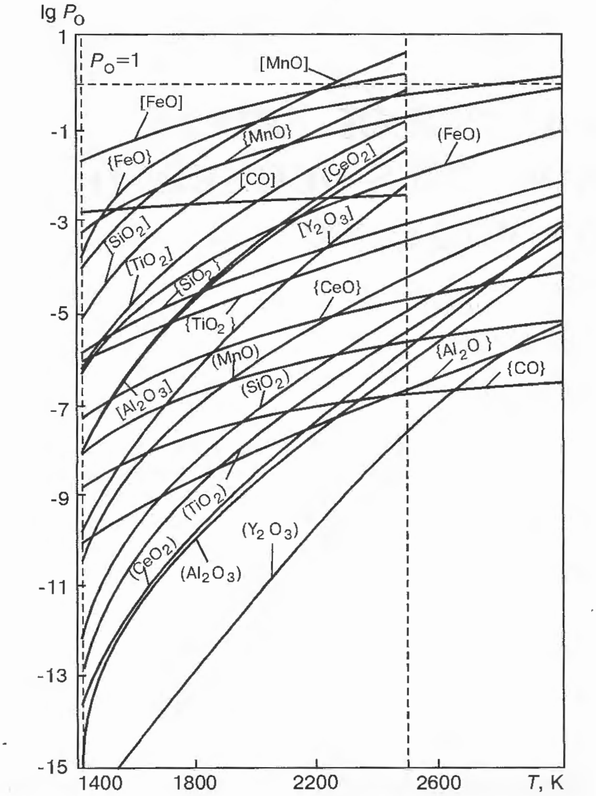

Figure 1. Temperature relation of specific mass constants of formation of oxides in three phases

At a given generalized diagram (Figure 1) of temperature relation of specific mass constants of formation of oxides in three phases, calculated per one gram-atom of oxygen, a partial pressure of oxygen $P_O = 10^5$ Pa corresponds to the value $\lg k_O = 0$. The physical meaning of this relationship consists in the fact that at temperature T_0 the equilibrium pressure of oxygen over oxide will be equal to external pressure of the 10^5 Pa pure oxygen, i.e. in the pure oxygen the metal will not be oxidized. The temperature T_0 will be calculated by formula

$$T_0 = \frac{A}{B}. \tag{4}$$

Analysis of curves (Figure 1) shows that with a temperature increase the dissociation pressure of all oxides, available in three phases: metal [...], slag (...) and gaseous {...} is increased. This indicates about decrease in stability of oxides, however, a free carbon and carbon, dissolved in a molten metal, remain the highest deoxidizing ability when high temperatures (> 2700 K) are reached.

To define the sequence of metallurgical processes in three phases it is rational to compare them using the same temperature. Table 1 gives reactions of formation of oxides of elements arranged by a degree of losses in an affinity to oxygen at the temperatures typical of the fusion welding.

Analysis of these reactions shows that, when the definite temperatures are attained, the carbon dissolved in a molten metal will deoxidize oxides of all deoxidizers, widely used in metallurgy, by their reduction up to pure elements and decreasing the content of non-metallic inclusions and oxygen in the deposited metal, as a gaseous oxide of carbon CO will be a product of the reaction. The same situation is observed in gaseous and slag phases.

Reduction of elements from carbon oxides. The burning-off of carbon in gas, slag and metal phases in fusion welding, as a result of interaction with oxygen of metal oxides, is a clearly expressed endothermal process occurring at high temperatures. Under the conditions of the arc welding the oxides can be deoxidized by carbon according to the reaction

$$MeO + C = Me + CO, \tag{5}$$

which is a result of two private reactions

$$2Me + O_2 = 2MeO, \tag{6}$$

$$2C + O_2 = 2CO. \tag{7}$$

Constant of equilibrium of the reaction of the carbon reduction of oxide (5) is an algebraic sum of reactions (6) and (7) of MeO and CO formation

$$\lg k_{MeO} = \frac{A_1}{T} + B_1, \tag{8}$$

$$\lg k_{CO} = \frac{A_2}{T} + B_2, \tag{9}$$

$$\lg k_{C/CO} = \lg k_{MeO} + (-\lg k_{CO}) = \frac{A}{T} + B, \tag{10}$$

where A_1, A_2, B_1, B_2 are the coefficients whose values are taken from tables of temperature relations $\lg k$ for corresponding reactions.

As CO is the only gaseous product of the reaction (5), the constant of equilibrium of the reaction

Table 1. Reactions of formation of oxides at temperatures in the zone of melting

T, K	*Series of probable sequence of formation of oxides in three phases*
1420	(Y_2O_3), (Al_2O_3), (CeO_2), (TiO_2), (SiO_2), (MnO), {Al_2O}, [Y_2O_3], {CO}, [CeO_2], [Al_2O_3], {YO}, {CeO}, {TiO_2}, (FeO), [TiO_2], [SiO_2], [MnO], {FeO}, {MnO}, [CO], [FeO]
1810	(Y_2O_3), (Al_2O_3), (CeO_2), (TiO_2), {Al_2O}, (SiO_2), {CO}, (MnO), {YO}, [Y_2O_3], {CeO}, {TiO_2}, [CeO_2], [Al_2O_3], {SiO_2}, (FeO), [TiO_2], [CO], [SiO_2], {MnO}, [MnO], {FeO}, [FeO]
2500	(Y_2O_3), {Al_2O_3}, {CO}, (Al_2O_3), (CeO_2), {YO}, (TiO_2), (SiO_2), {CeO}, (MnO), {TiO_2}, [CO], [Y_2O_3], {SiO_2}, (FeO), [Al_2O_3], [CeO_2], [TiO_2], {MnO}, {FeO}, [SiO_2]
3000	{CO}, {Al_2O}, (Y_2O_3), (Al_2O_3), {YO}, {CeO}, (TiO_2), (CeO_2), (SiO_2), (MnO), {TiO_2}, {SiO_2}, (FeO), {MnO}

Table 2. Results of calculation of temperature of beginning the reduction of oxides of main elements for three phases

Reaction	$T_{b.r}$		
$FeO + C = Fe + CO$	[1082]	(1060)	{668}
$MnO + C = Mn + CO$	[1587]	(1682)	{277}
$\frac{1}{2}SiO_2 + C = \frac{1}{2}Si + CO$	[1802]	(1941)	{586}
$\frac{1}{2}TiO_2 + C = \frac{1}{2}Ti + CO$	[2006]	(2040)	{700}
$\frac{1}{3}Al_2O_3 + C = \frac{2}{3}Al + CO$	[2236]	(2300)	–
$Al_2O + C = 2Al + CO$	–	–	{2773}
$\frac{1}{3}Y_2O_3 + C = \frac{2}{3}Y + CO$	[2483]	(2690)	–
$YO + C = Y + CO$	–	–	{788}
$\frac{1}{2}CeO_2 + C = \frac{1}{2}Ce + CO$	[2228]	(2181)	–
$CeO + C = Ce + CO$			{819}

$$k_{C/CO} = P_{CO}. \qquad (11)$$

The equilibrium pressure of CO, determined by this reaction, is a function of temperature.

The equilibrium of reactions of decarburization under the standard conditions (i.e. there are condensed independent phases MeO, Me, C and $P_{CO} = 10^5$ Pa) corresponds to the value $\lg k_{C/CO} = 0$, when $k_{C/CO} = P_{CO} = 1$.

Temperature, at which the reaction (5) is in equilibrium, is called a temperature of the beginning of carbon reduction of the metal oxide, i.e. $T_{b.r}$ [7]. The reaction (5) proceeding for the metal reduction is possible only at a real temperature T_r of metal oxide mixture with carbon which is above $T_{b.r}$, i.e. at $T_r > T_{b.r}$.

The $T_{b.r}$ value of the given oxide corresponds to the temperature at which the chemical affinity of the metal being reduced to oxygen becomes equal to the carbon affinity to the oxygen. If the carbon affinity at a definite temperature is higher than that of metal, the reaction (5) will proceed from left to right up to the establishing the CO equilibrium pressure. If the affinity of metal to oxygen is higher than that of carbon, then the reaction of metal oxidizing with a carbon oxide will proceed with a reduction of carbon.

The $T_{b.r}$ value can be found analytically from the equation of a constant of the decarburization reaction (10)

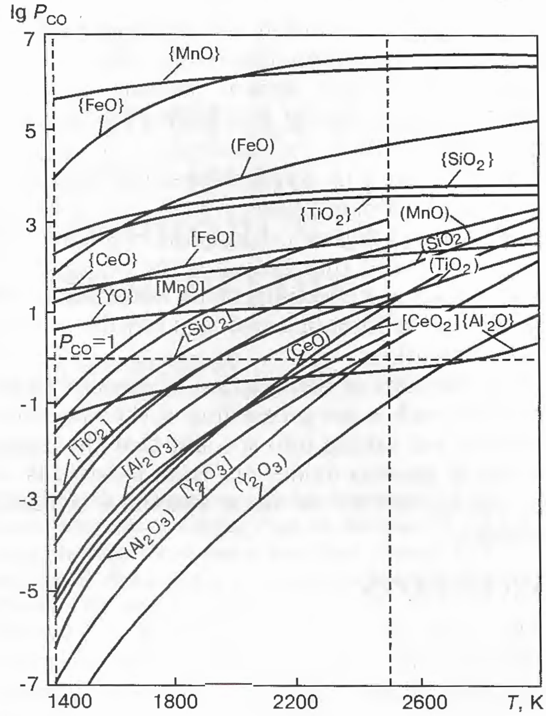

Figure 2. Temperature relation of constants of reactions of carbon reduction of main elements from oxides in three phases

$$\lg k_{C/CO} = \frac{A}{T} + B,$$

whence

$$T_{b.r} = \frac{A}{B}.$$

Figure 2 gives the temperature relation of constants of reactions of carbon reduction of main elements from oxides in three phases. Table 2 presents the results of calculation of values $T_{b.r}$ of oxides of main elements for gaseous, slag amd metal phases in fusion welding. Table 3 presents series of the probable proceeding of reduction reactions, arranged by the degree of losses in the chemical affinity of carbon to oxides at temperatures typical of the fusion welding.

From analyźing the results of calculation, given in Figure 2 and Tables 2 and 3, the conclusion can be made that in welding consumables which contain the high-carbon ferroalloys of Fe–C system the oxidation of dissolved carbon and reduction of iron, manganese and silicon from oxides is possible in heating within the 1420 – 1810 K temperature in-

[illegible]ries of probable proceeding of reactions of carbon reduction of elements from oxides in three phases

[illegible]	*Series of probable sequence*
1420	{MnO}, {FeO}, $\{SiO_2\}$, $\{TiO_2\}$, (FeO), {CeO}, [FeO], {YO}
1810	{MnO}, {FeO}, (FeO), $\{SiO_2\}$, $\{TiO_2\}$, [FeO], {CeO}, [MnO], (MnO), $[SiO_2]$
2500	{FeO}, {MnO}, (FeO), $\{SiO_2\}$, $\{TiO_2\}$, [MnO], {CeO}, [FeO], (MnO), $[SiO_2]$, (SiO_2), $[TiO_2]$, (TiO_2), (CeO), $[CeO_2]$, $[Al_2O_3]$, $[Y_2O_3]$, (Al_2O_3)
3000	{FeO}, {MnO}, (FeO), $\{SiO_2\}$, $\{TiO_2\}$, [MnO], (SiO_2), (CeO_2), {CeO}, (TiO_2), (Al_2O_3), {YO}, $\{Y_2O_3\}$, $\{Al_2O_3\}$

terval in case of exceeding the corresponding $T_{b.r}$. In a metal phase carbon can reduce also oxides of titanium, aluminium, zerium, yttrium and other elements during heating to 2500 K temperature.

In fusion welding the reactions of decarburization will proceed in three phases, but the values $T_{b.r}$ of oxides of manganese, silicon, titanium, aluminium and yttrium in a slag phase are higher than in a molten metal that indicates the preference in use of carbon as a deoxidizer in a bound state, for example, in the form of a cast iron powder or high-carbon ferroalloys.

The reactions of deoxidation of gaseous oxides with a free carbon are proceeding at the lower temperatures, but taking into account that the partial pressure of gaseous oxides in fusion welding is too low, the occurrence of these reactions is hardly probable.

CONCLUSIONS

1. The thermodynamic calculation of constants of equilibrium, reactions of formation of oxides and reactions of carbon reduction of elements of oxides in three phases is made. The generalized diagrams are plotted.

2. Series of a probable proceeding of reactions of oxidation of elements and carbon reduction of elements from oxides for typical temperatures of the zone of melting in arc welding are arranged.

3. Temperature of beginning the carbon reduction of oxides in a metal phase, except CeO_2 and FeO, is lower than that in a slag phase. This initiates the process of deoxidation at lower temperatures and gives a feasibility to use carbon in a bound state as a deoxidizer in welding consumables.

REFERENCES

1. Efimenko, N.G., Kalin, N.A. (1978) Deoxidizing ability of rare-earth elements as compared with known deoxidizers. *Svarochnoye Proizvodstvo*, **10**, 1 – 2.
2. Kokh, B.A. (1975) *Fundamentals of thermodynamics of metallurgical processes of welding*. Leningrad: Sudostroyeniye.
3. Kulikov, I.S. (1975) *Deoxidation of metals*. Moscow: Metallurgia.
4. Filippov, S.I. (1966) *Theory of metallurgical processes*. Moscow: Metallurgia.
5. Gulyaev, A.P. (1978) *Metals science*. Moscow: Metallurgia.
6. Pokhodnya, I.K. (1972) *Gases in welds*. Moscow: Mashinostroyeniye.
7. Kazachkov, E.A. (1988) *Calculations related to the theory of metallurgical processes*. Moscow: Metallurgia.

PECULIARITIES OF PHASE AND STRUCTURAL TRANSFORMATIONS OCCURRING IN GRAY CAST IRONS WITH A DIFFERING PHOSPHORUS CONTENT DURING THERMAL-DEFORMATION WELDING CYCLE

G.M. KROSHINA, V.G. VASILIEV and **D.P. NOVIKOVA**
The E.O. Paton Electric Welding Institute, NASU, Kyiv, Ukraine

ABSTRACT

Phase and structural transformations in commercial cast iron SCh20 with a phosphorus content of 0.10 and 0.28 % during welding have been investigated. The effect of the thermal-deformation welding cycle on deformability of cast irons has been studied. Continuous cooling transformation diagrams for austenite have been plotted. It is shown that an increased phosphorus content of gray cast iron favours development of an intermediate transformation of austenite in the HAZ metal. Peculiarities of behaviour of phosphide eutectic during the thermal-deformation welding cycle have been investigated.

Key words: *fusion welding, gray cast irons, thermal-deformation welding cycle, phase transformations, microstructure, phosphide eutectic, continuous cooling transformation diagram, transformation of austenite, cooling rate, graphite inclusions.*

Thin-walled castings ($\delta = 5 - 15$ mm) of gray cast iron SCh20 with a phosphorus content of 0.10 % have wide commercial application. Structure and mechanical properties of such cast irons exhibited during the thermal-deformation welding cycle are well studied [1 – 4]. An increase in the phosphorus content of up to 0.30 % is reported [5] to lead to a decrease in size of the eutectic grain of metal of the above castings. Also, this makes the metal structure isotropic through the thickness, which causes an increase in cast iron strength and wear resistance. However, almost no literature data are available on the effect of the thermal-deformation welding cycle on peculiarities of formation of structure of the HAZ of a commercial gray cast iron with a phosphorus content of up to 0.30 %. The only data available refer to ESR gray cast iron with P = = 0.28 % [6]. In this connection of interest are comparative investigations of phase and structural transformations occurring in commercial gray cast irons of the SCh20 grade with P = 0.10 – 0.28 % and study of behaviour of the phosphide eutectic (PE) during the thermal welding cycle.

The authors conducted investigations on samples of SCh20 with a phosphorus content of 0.10 and 0.28 % and an almost equal mass fraction of other elements. Critical points of the cast irons under investigation were determined using the Chevenard dilatometer, and solidification temperature ranges were estimated using the VDTA-8M installation (Table 1). Size and distribution of the graphite phase, as well as characteristic peculiarities of PE were evaluated in compliance with GOST 3443–87. To provide the identical structure, the samples were preliminarily subjected to high-temperature annealing (T_h = 900 °C, holding for 2 h and air cooling). Structure of the investigated cast iron samples is shown in Figure 1. Kinetics of transformation of austenite in the HAZ was studied using the fast-response dilatometer developed by the E.O. Paton Electric Welding Institute [7], and derivative thermal analysis was done using the instrument developed by the Slovakian Research Institute of Welding [8]. The object of investigation was cast iron with a shape of graphite characteristic of thin-walled castings, therefore, in our investigations we reproduced actual thermal cycles prac-

Table 1. Chemical composition and critical points of cast iron SCh20 under investigation

No. of sample	*Content of elements, wt.%*						*Critical points, °C*			
	C	*Si*	*Mn*	*Cr*	*P*	*S*	T_s	T_l	A_{c1}	A_{c3}
1	3.20	2.00	0.72	0.23	0.10	0.120	1150	1190	760	820
2	3.27	2.20	0.54	0.23	0.28	0.013	1115	1170	780	830

© G.M. KROSHINA, V.G. VASILIEV and D.P. NOVIKOVA, 2000

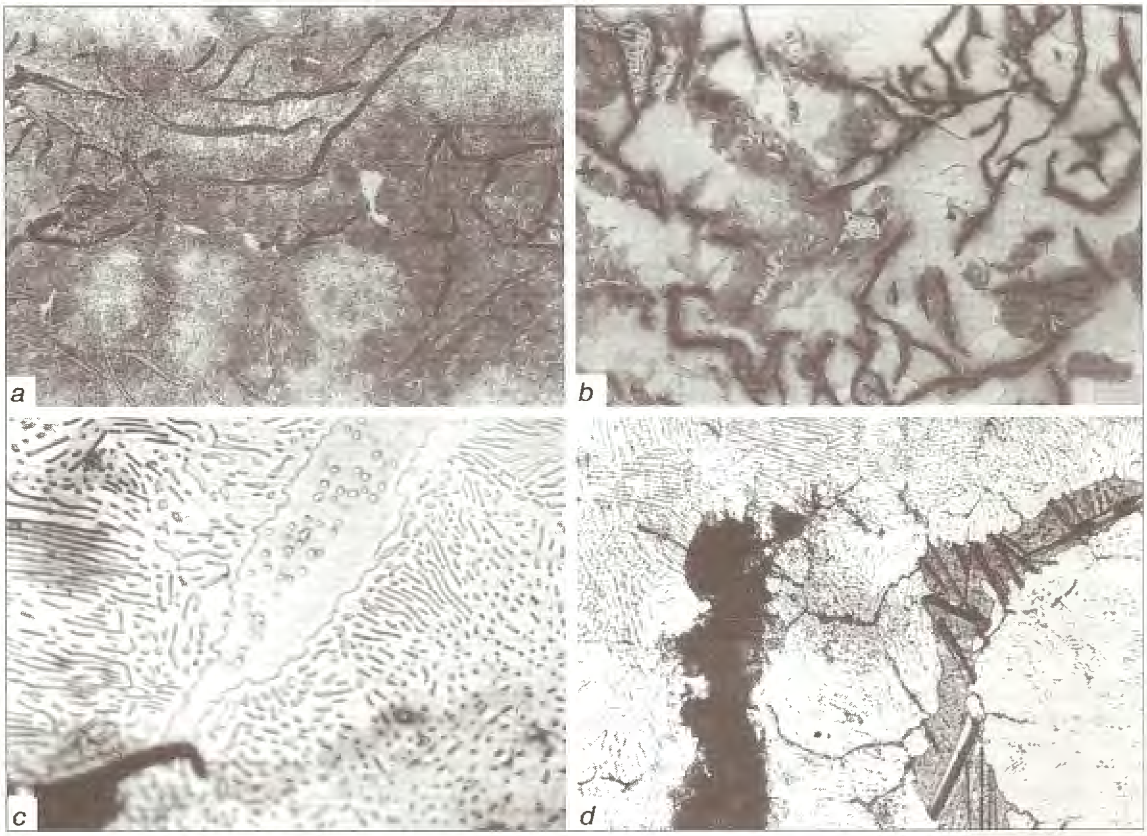

Figure 1. Microstructure of gray cast irons SCh20 with P = 0.10 (*a*) and 0.28 % (*b*) (×150), containing PE1 (*c*) (×800) and PE5 (*d*) (×650) (reduced by 7/10)

ticed in welding repair of casting and service defects in thin-walled parts made from SCh20 [9].

Two regions of the HAZ were investigated: one heated to a temperature below the solidus point (about 1100 °C) and the other — heated to a temperature above the critical point of A_{c3} (900 °C). These are the main regions which are most responsible for the quality of a welded joint. Structure and deformability of the cast irons were investigated within the same temperature range (900 – 1100 °C). Investigations of the kinetics of transformation of overcooled austenite involved comprehensive analysis of dilatometric and thermal curves of cooling. Microstructure of the simulation samples was studied by optical metallography using the «Neophot» microscope. Distribution of phosphorus and silicon in the cast iron matrix and PE was determined by X-ray spectrometry using the CAMECA installation MS-46. The «ALA-TOO» high-temperature metallography installation was used to study the effect of the welding thermal cycle on deformability of the cast irons. Tensile tests were carried out on standard specimens with a cross section of 3 × 3 mm and 70 mm long at temperatures of 900, 1000 and 1100 °C, as well as during subsequent cooling under conditions of a maximum possible deformation which does not lead to complete fracture of the metal. The minimum stress values at which an instantaneous fracture occurs were determined by selection of the load for each test temperature. The test procedure employed is described in [10].

As shown by the results obtained, the matrix of the SCh20 cast iron with P = 0.10 % consists mostly of pearlite, the ferrite content being 10 % (Figure 1, *a*). Binary PE (PE1) has an area of 6000 – 8000 μm^2 (Figure 1, *c*). There are also individual inclusions of ternary PE with cementite laminae (PE5), the area of which is 800 – 1000 μm^2 and the length of the graphite inclusions is 220 – 250 μm (Figure 1, *d*). The graphite phase has an inter-dendrite distribution.

The SCh20 cast iron with P = 0.28 % has a ferritic-pearlitic structure with a ratio of the pearlite and ferrite components equal to 50:50 (Figure 1, *b*), i.e. it contains a larger amount of ferrite than the cast iron with P = 0.10 %. The area of PE1 is 800 – 1000 μm^2 (Figure 1, *c*) and that of PE5 is 10000 – 12000 μm^2 (Figure 1, *d*). PE5 has some specific features described in [11]. They are not classified in GOST 3443–87 and consist in the fact that there are thinned regions in the form of «whiskers» and individual embedments of cementite near PE, as well as phosphides in the bulk of the matrix regions adjoining it. The graphite inclusions are 250 – 280 μm long. The graphite phase also has an inter-dendrite distribution. It should be noted that PE is always located in the dendrite

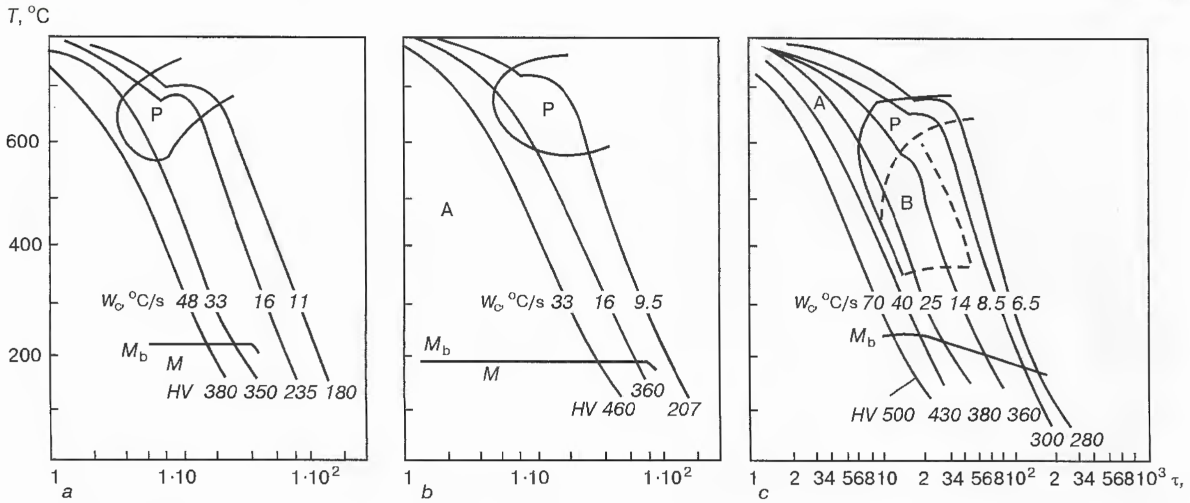

Figure 2. Austenite continuous cooling transformation diagrams at W_h = 150 °C/s plotted for cast iron with P = 0.10 (*a, b*) and 0.28 % (*c*) at T_h = 900 (*a*) and 1100 °C (*b, c*)

spacings between the axes in the form of individual inclusions, as indicated in [11].

To plot the austenite continuous cooling transformation diagrams the samples were heated at a rate of W_h = 150 °C/s to a temperature of 900 and 1100 °C, and then cooled in accordance with the thermal welding cycle. The austenite continuous cooling transformation diagrams were almost identical for the SCh20 cast irons with a phosphorus content of 0.10 and 0.28 % in heating to a temperature of up to 900 °C.

Based on the data of the diagram (Figure 2, *a*) [2], at W_c < 16 °C/s the austenitic transformation occurs within an upper temperature range of 740 – 670 °C, while at W_c > 16 °C/s it occurs not only within this range but also within the martensite region (the temperature of beginning of the martensitic transformation is M_b = 220 °C).

The austenite continuous cooling transformation diagrams for the SCh20 cast irons with a phosphorus content of 0.10 and 0.28 % at T_h = 1100 °C are shown in Figure 2, *b, c*.

In the cast iron with P = 0.10 % at W_c = = 9.5 °C/s the transformation occurs within the upper temperature range of 745 – 595 °C. The structure is a ferrite-carbide mixture and hardness of the matrix is *HV* 207. At W_c = 16 °C/s the austenitic transformation occurs both in the upper and lower temperature range. M_b = 190 °C. It should be noted that at such cooling rates the nonhomogeneity of austenite increases. In the PE precipitation regions there are zones of the ferrite-carbide mixture, most often they are of a globular shape (Figure 3, *a*). Hardness of the matrix is up to *HV* 360. At W_c ≥ 33 °C/s the austenitic transformation occurs only in the martensitic region (Figures 2, *b* and 3, *b*), and hardness of the matrix increases to *HV* 460.

In the cast iron with P = 0.28 %, in heating to 1100 °C and at W_c = 6.5 – 8.5 °C/s, austenite is sufficiently stable. Its transformation begins at 690 °C and occurs mostly in the upper temperature range of up to 640 °C and, moderately, in the martensitic range (M_b = 170 – 180 °C). Structure of the matrix which has hardness of *HV* 280 – 300 consists of pearlite of a differing degree of dispersion and individual martensitic regions. Their formation in the pearlitic matrix during cooling is probably aided by an increased carbon content of

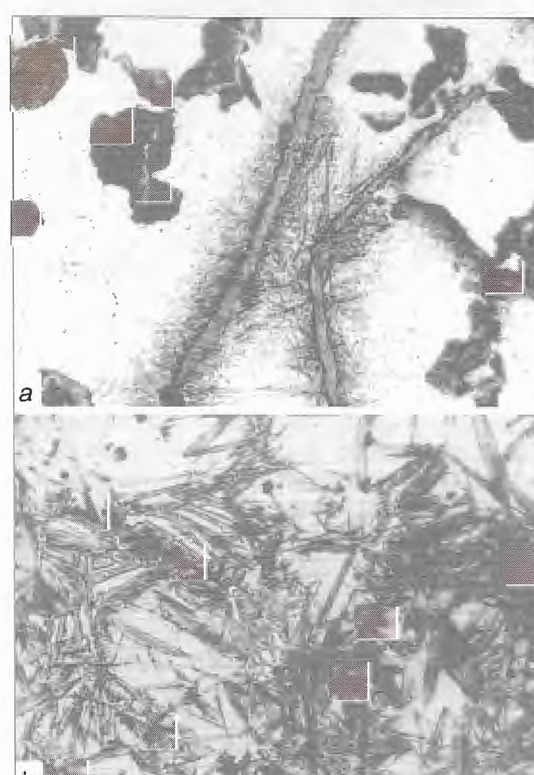

Figure 3. Microstructure of samples of cast iron with P = 0.10 % at T_h = 1100 °C and W_c = 16 (a) (×600) and 33 °C/s (*b*) (×800) (redused by 0.75)

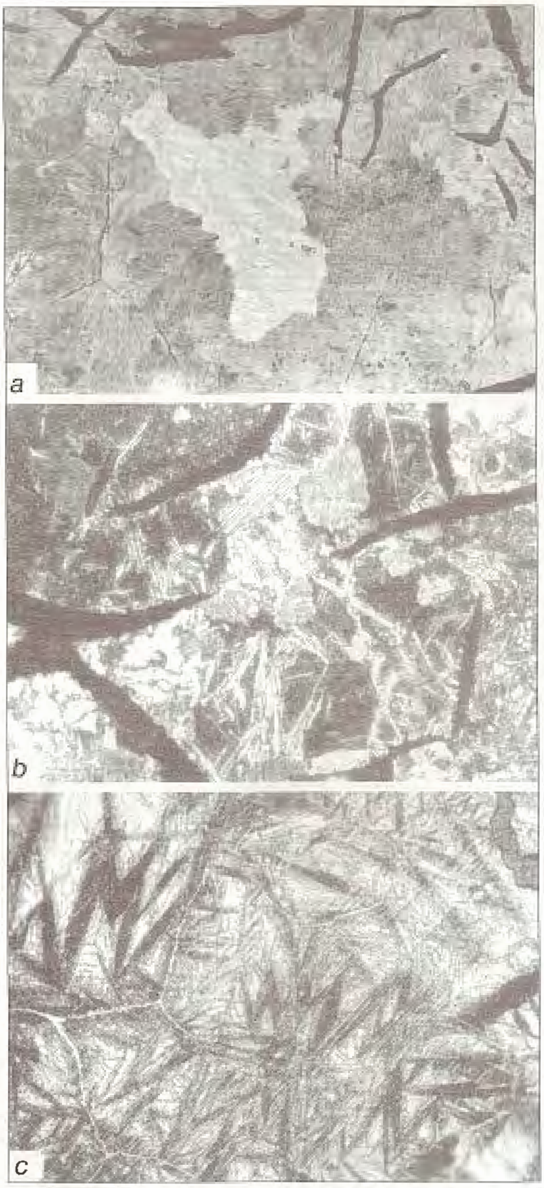

Figure 4. Microstructure of samples of cast iron with P = 0.28 % at T_h = 1100 °C and W_c = 6.5 – 8.5 (*a*), 14 – 40 (*b*) (×600) and 70 °C/s (*c*) (×800) (reduced by 7/10)

some austenitic regions (Figure 4, *a*). The austenitic transformation at W_c = 14 – 40 °C/s occurs in the upper and middle temperature range from 650 – 500 to 380 °C and in the martensitic region (Figures 2, *c* and 4, *b*). Hardness of the matrix at W_c = 14 – 25 °C/s is *HV* 360 – 380, the content of the martensitic phase is 15 – 20 %; at W_c = 40 °C/s the content of the martensitic component amounts to 35 – 40 % and hardness of the matrix is *HV* 430. At $W_c \geq$ 70 °C/s the austenitic transformation occurs only in the martensitic region (Figures 2, *c* and 4, *c*) and hardness of the matrix increases to *HV* 480 – 520. In this case the time difference in the formation of martensite (martensitic needles have dark and light colouring) also seems to be associated with the non-homogeneity of austenite.

In the cast iron with P = 0.28 % each cooling rate corresponds to a certain value of temperature M_b – 180, 210, 230 and 240 °C at W_c = 8.5, 14, 25 and 40 °C/s, respectively. This floating point of beginning of the martensitic transformation is probably associated with a wide range of temperatures of the preceding intermediate transformation (Figure 2, *c*). Shift of the martensitic transformation beginning in the case of a wide intermediate transformation range for high-strength steels was considered by A.M. Makara in [12].

Despite contradictions in the available data on the effect of phosphorus on the temperature range and character of phase transformations in medium-alloyed steels and gray cast irons [13 – 16], the authors do not disagree that phosphorus causes a substantial widening of the temperature range between liquidus and solidus. This is known to favour development of primary segregation and narrowing of the γ-region and, hence, retention of segregation in the solid state. Our experimental data coincide with conclusions of the authors of [13 – 16] that at an increased carbon content phosphorus promotes overcooling of austenite.

As shown in Figure 2, in the SCh20 cast irons at P = 0.10 % the austenitic transformation begins at a temperature of 745 °C and at P = 0.28 % this temperature decreases to 698 °C. During the $\gamma \to \to \alpha$ transformation, when the crystalline lattice of iron undergoes restructuring, the bond between phosphorus and silicon atoms and iron is violated, which causes these atoms to diffuse into ferrite [6]. Chemical heterogeneity in phosphorus and silicon formed during solidification favours the formation of ferrite with a differing silicon content. Phosphorus and silicon are the analogue elements that expand the α-region. As the silicon content of the cast iron is much higher than the phosphorus content, the effect of silicon is dominant. In our investigations the cast iron with P = 0.28 % (at T_h = = 1100 °C and W_c = 0.6 – 25.0 °C/s) also exhibits individual regions of ferrite with a differing silicon content. Redistribution of carbon, phosphorus and silicon within the critical temperature range has a substantial effect on the temperature of the austenitic transformation in the upper temperature range for iron-carbon alloys. It is clear from the abovesaid that our experimental results are in agreement with the literature data.

It should be noted that at T_h = 1100 °C these cast irons are characterized by peculiar processes of melting and subsequent solidification of PE. Regions of the matrix around PE5, which in the initial state contains phosphide, ferrite and cementite, are enriched at this temperature with phosphorus in the cast iron with P = 0.10 % at W_c = 16 – 25 °C/s

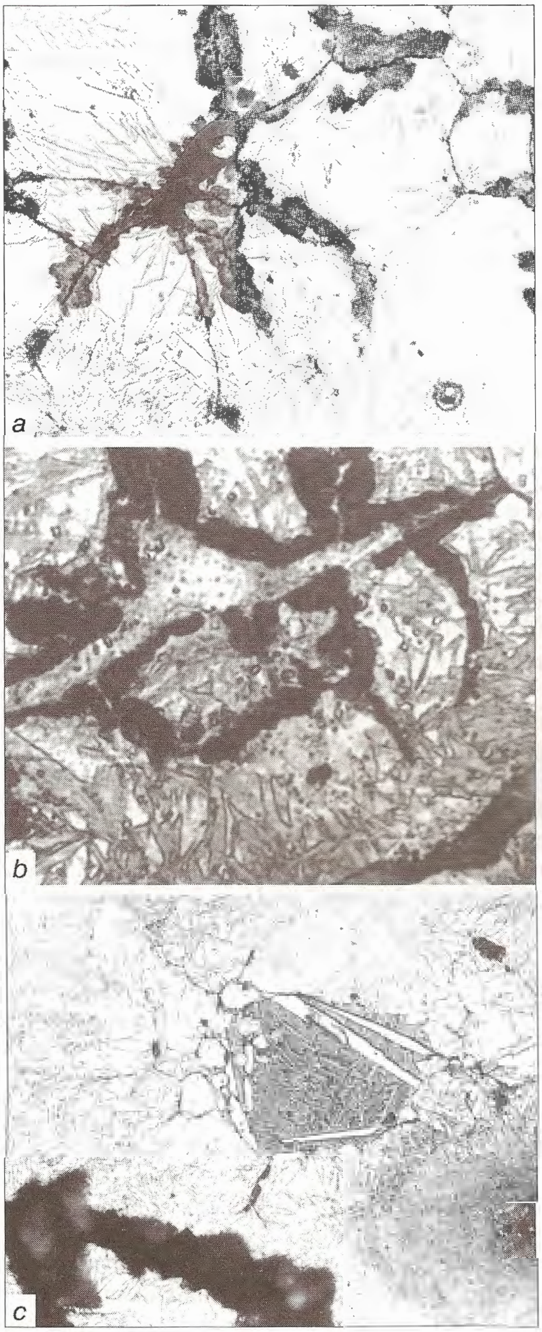

Figure 5. Variations in microstructure and configuration of PE in the matrix regions adjoining it at T_h = 1100 °C in cast irons with P = 0.10 % at W_c = 16 – 25 °C/s (a) (×600), P = 0.28 % at W_c = 8.5 – 40.0 °C/s (b) (×800) and P = 0.10 % at W_c = = 33 °C/s (*c*) (×600) (reduced by 4/9)

and in the cast iron with P = 0.28 % at W_c = 8.5 – 40.0 °C/s. This is evidenced by the distribution of basic elements in binary and ternary PE and the adjoining regions of the matrix [11]. The phosphorus content of these regions of the cast iron with P = 0.10 and 0.28 % is 0.2 – 0.5 and 0.2 – 0.8 %, respectively. This is attributable to the fact that during the $\gamma \rightarrow \alpha$ transformation (at a high carbon content of the matrix) there is a strong antagonism between carbon and phosphorus [14]. Since carbon

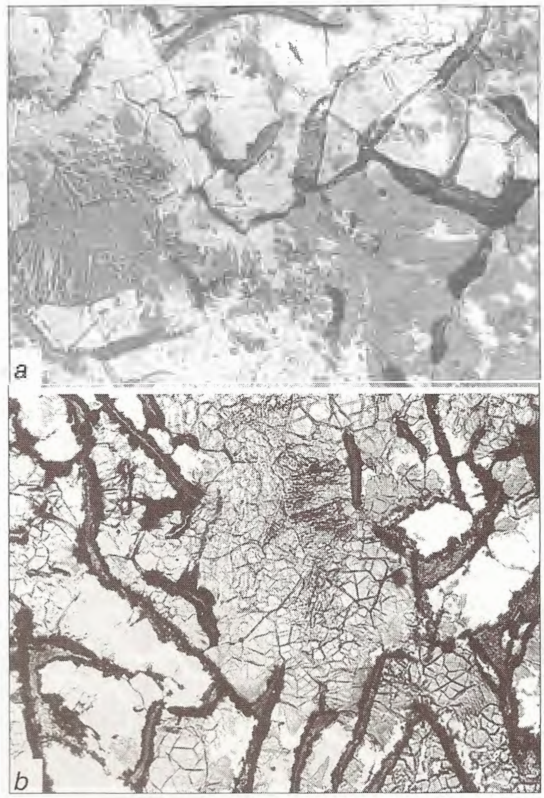

Figure 6. Effect of deformation on microstructure of cast iron with P = 0.10 % at T_h = 1000 °C (a) and P = 0.28 % at T_h = = 1100 °C (*b*) (×400) (reduced by 3/5)

is an austenite former and phosphorus is a ferrite former, the rate of diffusion of phosphorus into the solid phase and that of carbon into the liquid phase are increased. It is probable that after the formation of the liquid phase (at T_h = 1100 °C) carbon diffuses into it from the boundary regions of the solid phase (austenite) enriched with phosphorus. As above said, the interfaces are formed near the incipiently melted grain boundaries and the phosphorus-rich matrix, where the austenitic transformation occurs in the upper temperature range. Structure of these regions is a ferrite-carbide mixture having a differing degree of dispersion (Figure 5, *a*). Regions in which such processes occur take about 15 % of the total area. In the cast irons investigated the PE regions (with an area of 400 – 600 μm^2), which in the initial state contain ferrite and phosphide, are melted at T_h = 1100 °C and W_c = 8.5 – 40.0 °C/s. Phosphorus diffuses from these volumes of the liquid phase into the surrounding solid matrix to cause phosphorus enrichment of these regions on their perimeter, this initiating the austenitic transformation to occur in the upper temperature range. This postulate has an experimental proof.

As shown by metallography and X-ray spectrometry, structure of these regions is a dispersed ferrite-carbide mixture (Figure 5, *b*). The phosphorus content of these regions is 0.2 – 0.7 %, while that in the prior PE locations is 0.10 – 0.28 %, which corresponds to the phosphorus content of

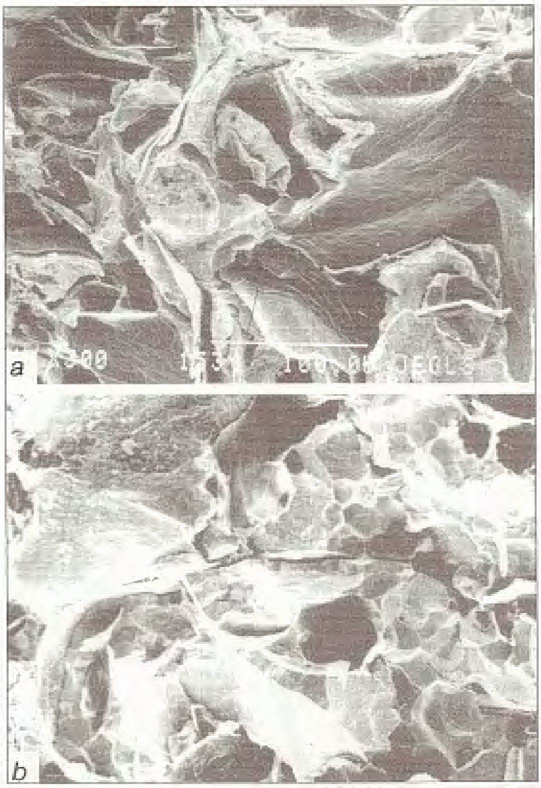

Figure 7. Fractogram of the fracture surface in cast irons with P = 0.10 % after heating at W_h = 150 °C/s to 1000 °C and at W_c = 33 °C/s (*a*) (×300), with P = 0.28 % after heating at the same rate to 1100 °C and at W_c = 40 °C/s (*b*) (×600) (reduced by 7/10)

the cast iron matrix. In the cast iron with P = = 0.10 % at W_c > 33 °C/s and cast iron with P = = 0.28 % at W_c = 70 °C/s, both PE1 and PE5 predominantly preserve their form (Figure 5, *c*).

The deformability investigations showed that the samples of gray cast iron with P = 0.10 % could withstand a certain deformation level only at T_h = = 900 and 1000 °C, and the samples of gray cast iron with P = 0.28 % could bear this deformation at all test temperatures without fracture (Table 2). The maximum ductility of both cast irons was fixed in heating to 900 °C, which seems to be associated with the $\alpha \rightarrow \gamma$ transformation and formation of the austenitic matrix. Elongation of the cast iron samples with P = 0.28 % is larger than that of the cast iron with P = 0.10 % (Table 2). With an increase in the test temperature to 1000 °C a decisive role in fracture of the samples is played by the graphitization processes which lead to porosity and then discontinuities formed in the cast iron matrix (Figure 6, *a*). Similar phenomena are described in [17]. Fracture in SCh20 with P = 0.10 % occurs after the matrix exhausts its safety factor for ductility at 1000 °C. At this temperature no fracture centres are observed in the cast iron with P = = 0.28 %. They appear at T_h = 1100 °C. This is associated with the processes which occur in the cast iron matrix. In particular, these are the graphitization process leading to discontinuities and process of grain boundary slip along the forming subgrains (Figure 6, *b*). It should be noted that fracture of the cast iron matrix at T_h = 1100 °C and W_c = 33 °C/s in SCh20 with P = 0.10 % occurs in the graphite phase, resulting in the formation of characteristic brittle fracture with a groove-like pattern (Figure 7, *a*), and in SCh20 with P = 0.28 % at W_c = 40 °C/s fracture is of a mixed character, the grain boundary fracture taking approximately 30 % (Figure 7, *b*). The investigations conducted showed that the cast iron with P = 0.28 % has higher strength and ductile characteristics. This is attributable to the fact that the transformation of austenite in the range of temperatures of its maximum stability (800 – 500 °C), at W_c = 40 °C/s corresponding to conditions of mechanized welding of thin-walled parts with a heat input of 5 – 8 kJ/cm, occurs to form a ferrite-carbide mixture in the upper and middle temperature ranges, whereas in the cast iron with P = 0.10 % at the same cooling rate it occurs only in the martensitic region.

Table 2. Mechanical properties of samples of gray cast irons SCh20

Sample No.	T_{test}, °C	*Tensile strength, MPa*	*Elongation, mm*
1	900	20	8.0
	1000	5	0.4
2	900	32	15.0
	1000	15	0.6
	1100	1	0.3

CONCLUSIONS

1. An increase in the phosphorus content has a fundamental effect on the kinetics of transformation of austenite in the HAZ. The continuous cooling transformation diagram shows that if in SCh20 with P = 0.10 % the austenitic transformation occurs only in the pearlitic and martensitic regions, at P = 0.28 % the developed bainitic region is formed.

2. In a temperature range of 800 – 500 °C, at W_c = 40 °C/s corresponding to the conditions of mechanized welding of thin-walled parts without preheating at a heat input of 5 – 8 kJ/cm, the austenitic transformation in the HAZ of the cast irons with P = 0.10 % occurs only in the martensitic region, while in that with P = 0.28 % it occurs in the upper and intermediate regions to form a ferrite-carbide mixture (75 – 80 %) and martensite (20 – 25 %).

3. At the same temperatures and cooling rates the strength and ductility values of the HAZ of the cast iron with P = 0.28 % are higher than those of the cast iron with P = 0.10 %.

REFERENCES

1. Granjon, H. (1971) Soudabilite des fontes a la lumiere des diagramme de transformation au refroidissement continu. *Soudage et Techniques Connexes*, **1/2**, 7 – 15.
2. Gretsky, Yu.Ya., Vasiliev, V.G., Kroshina, G.M. (1979) Formation of structure of the HAZ in welding of gray pearlitic cast iron. *Avtomaticheskaya Svarka*, **1**, 22 – 25.
3. Gretsky, Yu.Ya., Kroshina, G.M., Shekera, V.M. (1980) Mechanical properties of the HAZ after welding of structural cast irons. *Ibid*., **1**, 71 – 72.
4. Gretsky, Yu.Ya., Novikova, D.P., Kroshina, G.M. (1986) Strength and ductility of pearlitic cast irons at temperatures characteristic of the HAZ during welding. *Ibid*., **3**, 15 – 18.
5. Khrapkovsky, E.Ya. (1965) *Structure and strength of thin-walled castings of gray cast iron*. Moscow: Mashinostroyeniye.
6. Kroshina, G.M., Vasiliev, V.G., Novikova, D.P. *et al.* (1996) Effect of phosphorus and thermal-deformation welding cycle on structure and properties of ESR gray cast iron. *Avtomaticheskaya Svarka*, **1**, 10 – 17.
7. Vasiliev, V.G., Malevsky, Yu.B. (1981) Dilatometer for investigation of phase transformations during the thermal welding cycle. In: *Physical methods for investigation of metals*. Kyiv: Naukova Dumka.
8. Shtembera, B., Mraz, L. (1981) Investigation of phase transformations and plotting the austenite decomposition diagrams for the weld metal by the direct method. *Svarochnoye Proizvodstvo*, **4**, 5 – 8.
9. Gretsky, Yu.Ya., Melnichenko, I.M. (1979) Thermal cycles in arc welding of thin-walled cast iron parts. *Avtomaticheskaya Svarka*, **11**, 23 – 26.
10. Novikova, D.P. (1989) *High-temperature metallography of welded joints*. Kyiv: Naukova Dumka.
11. Kroshina, G.M., Grigorenko, G.M., Tikhonovskaya, L.D. *et al.* (1989) Effect of thermal cycle on structure of phosphide eutectic in gray cast irons. *Avtomaticheskaya Svarka*, **12**, 44.
12. Makara, A.M., Novikova, D.P. (1967) Peculiarities of martensitic and bainitic transformations in alloyed steels during thermal-deformation welding cycles. *Avtomaticheskaya Svarka*, **10**, 10 – 15.
13. Gudremon, E. (1966) *Special steels*. Moscow: Metallurgia.
14. Kantorovich, I.E. (1948) *Heat treatment of steel and cast iron*. Sverdlovsk: Metallurgizdat.
15. Bogachev, I.N. (1962) *Metallography of cast iron*. Sverdlovsk: Metallurgizdat.
16. Girshovich, N.G. (1966) *Solidification and properties of cast iron in the form of castings*. Moscow: Mashinostroyeniye.
17. Ohide, T.G. (1975) The effect of annealing cycles on the graphitization of white cast iron. *AFS Cast Metals Res. J.*, **3**, 69 – 76.

IMPROVEMENT OF PROCESS OF CONSUMABLE ELECTRODE WELDING WITH AN INTERMITTENT ARC

A.T. NAZARCHUK
The E.O. Paton Electric Welding Institute, NASU, Kyiv, Ukraine

ABSTRACT

Some basic schematics are analyzed of stabilization of arc excitation and running in metal-electrode arc welding with weld formation in portions, in particular using a low-amperage arc. Shown is the rationality of making up the welding circuit of several independently controlled loops which provide the conductance of the arc gap, main arc running, control of the capacitor discharge in the arc gap by means of capacitive or inductive contours connected directly into the welding circuit.

Key words: arc welding, welding arc, arc exiting, arc stability, stability, pilot arc, portion heat input, welding circuit, investigations.

Portion formation of welds in a consumable electrode welding widens greatly the technological potentiality of the mentioned method of welding [1 – 3]. The development of new methods of a pulsed-arc welding is an important stage in the development of this trend [4 – 8].

The process of the tungsten electrode pulsed-arc welding using a «pilot» arc was created long ago [5]. A pilot low-amperage arc is designed for stabilizing repeated excitations and burning of the main welding arc in a pulsed condition.

In the pulsed-arc consumable-electrode welding the current pulsations are made as regards to a background current of a definite value [6, 7]. As to other schemes of pulsations of the basic current with respect to a background current [6, 7], then they provide the use of high-frequency pulsations mainly (up to 300 Hz). In our case the low-frequency pulsations (less than 0.5 Hz) are used, when not only frequency of pulsations, but also the duration of pulses and pauses have a decisive effect on the weld metal solidification and thermodeformational cycles of welding [1 – 3].

The present work is aimed at analyzing the schemes of stabilization of exciting and burning of

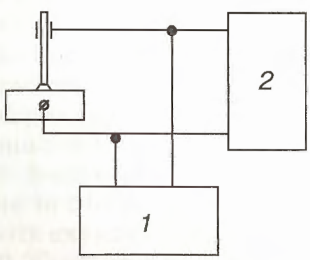

Figure 1. Schematic diagram of welding circuit for stabilizing the process of welding with a portion formation of weld: *1* — unit for a pilot arc supply; *2* — unit for a main arc loop supply

© A.T. NAZARCHUK, 2000

arc in consumable electrode welding providing a portion formation of welds [1 – 3] and also at the development of procedures which widen the technological capabilities of arc, first of all, in welding with a portion heat input.

It is known that application of a pulsed arc is especially effective in that case when the weld consists of separate mutually overlapping volumes (portions) of metal, providing an intermediate solidification of each of them before the next one [1, 2]. To realize this condition within the wide range of conditions of a consumable electrode welding, the pause between two related periods of arc burning should be approximately 3 – 5 s, and for a repeated excitation of the welding arc the reliable methods should be used.

For this purpose an auxiliary low-amperage arc, burning continuously during the whole process of welding was used, unlike the main arc which is burning in the pulsed condition.

The schematic diagram of the above-mentioned process of welding is presented in Figure 1. The power source of the auxiliary (pilot) arc supply is made in such a way that to provide a stable burning of the low-amperage arc at the currents at which the consumable electrode is not almost melted during a pause. Here, the arc should preserve a possibility of a maximum elongation and stable burning at voltages which exceed those of the main arc. The fulfilment of these conditions and rational combination of the duration of switching-off of the main arc and feeding the welding wire (with allowance for an inertia of the feeding mechanism) will provide a reliable repeated exciting of the main arc after each pause.

The similar scheme of stabilizing the arc excitation with a portion-discrete weld formation was also used in the manual arc welding. Experiments showed its high effectiveness. Moreover, during the manual arc welding the interrupted burning of the main arc can be often realized without a special

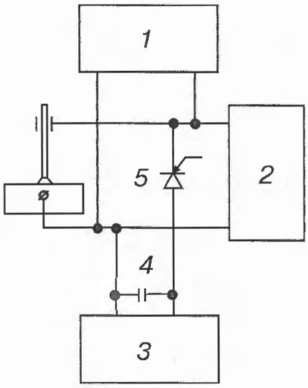

Figure 2. Arrangement of welding circuit of three independently-controlled loops (auxiliary and main arcs and capacitive loop): *1* — unit for supply arc which provides the arc gap conductivity; *2* — the same of the main arc; *3* — the same of a bank of capacitors; *4, 5* — thyristor key

device, only at the expense of an elongation of the arc gap. We think, that this feature can be widely used in the manual arc welding in different spatial positions.

During the experiments on the manual arc welding using a low-amperage pilot arc, it appeared feasible to use a power source with a rigid characteristic to supply the main arc. This circumstance and also an admissible decrease in an open-circuit voltage can reduce the consumption of electric energy, consumed by the main power source due to decrease in an inner drop of the voltage.

In arc welding with a consumable electrode a large attention is paid to a mass transfer of the electrode metal through the arc gap. To provide an additional effect on the mass transfer we used an independent loop (Figure 2) designed for charging the bank of capacitors, whose an organized discharge through the arc gap is controlled by a special thyristor key. The application of an independent source for this purpose makes it possible to control the voltage of charging the capacitors.

It should be noted that the inductive-capacitive loops in welding circuits are used for a long time. The most widely-spread scheme, used by us, is presented in Figure 3.

In resistance capacitor-type welding a controllable discharge of the capacitors is used to the welding circuit. However, we have also selected an independently controlled discharge of capacitors directly to the arc gap. This provided a uniform melting and transfer of the electrode metal at low welding currents (for example, for 4 mm diameter electrodes the current was approximately 25 A).

In regard to control the discharge of capacitors to the arc gap it is worthy to note the following. Block-diagram, presented in Figure 3, does not envisage an independent control of the capacitor discharge to the arc gap, feasible according to the block-diagram, given in Figure 2.

In general, the low-amperage pilot arc can be considered as an arc which provides the conductivity of the arc gap, especially in those cases when the power source of the main arc does not guarantee the existence of the arc process when the low-amperage pilot arc is switched off. This is typical of the manual arc welding with coated electrodes using transformer with a rigid characteristic and also in case of using a controllable discharge of the capacitor to the arc gap. As an example, when the voltage of the capacitor is insufficient for a breakdown of the interelectrode gap, then a low-amperage arc is used to provide its conductivity.

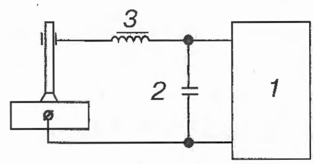

Figure 3. Most widely-spread schematic diagram of a capacitance connection in fusion arc welding: *1* — arc power source; *2* — bank of capacitors; *3* — choke

We suppose, that the use of a controllable discharge of the capacitors directly to the arc gap will be also reasonable in welding with a non-consumable electrode, and also in surfacing, for example, small-diameter bodies of rotation.

It should be noted in conclusion that during welding with a portion formation of welds the arrangement of the circuit using independently controlled loops where each of them fulfills its functional purpose makes it possible to widen the technological capabilities of the mentioned method, to reduce the consumption of energy. Nevertheless, it is necessary to consider development of welding arc supply sources of the new type. Concerning functional purposes of each of the loops, it is possible to distinguish the ensuring of the conductivity of arc gap and required heat capacity of the welding arc which is burning in stationary or pulsed conditions; control of electrode metal transfer and other characteristics of the welding process.

CONCLUSIONS

1. To stabilize the arc exciting and burning during a consumable electrode welding with a portion formation of welds it is necessary to use a low-amperage auxiliary («pilot») arc which provides conductivity of the arc gap, but does not almost participate in the electrode melting.

2. To widen the technological capabilities of the welding arc it is rational to make the welding circuit multiloop, for example, of three independently-controlled loops which provide a stable burning of a low-amperage arc, burning of the main arc of the required power, independent control of discharge of capacitors in the arc gap using a capacitive or inductive loop connected directed to the welding circuit.

3. The realization of the process of welding using a low-amperage «pilot» arc and main arc supplied from the power source with a rigid characteristic

will reduce the consumption of the electric energy due to decrease in losses, used for creation of the falling characteristics, where they are the necessary condition for the welding arc existence and fulfilment of the process of welding.

REFERENCES

1. Nazarchuk, A.T., Lipodaev, V.N. *Method of arc welding*. USSR author's certificate **1818180**, Int. Cl. B 23 K 9/16. Publ. 30.05.93.
2. Hazarchuk, A.T. (1994) Control of weld metal solidification and thermodeformational cycle in automatic arc welding. *Avtomaticheskaya Svarka*, **5 – 6**, 3 – 9.
3. Nazarchuk, A.T. (1997) Effect of portion-discrete formation of welds on thermal cycle of fusion arc welding. *Ibid.*, **5**, 13 – 17.
4. (1974) *Technology of electric fusion welding of metals and alloys*. Ed. by B.E. Paton. Moscow: Mashinostroyeniye.
5. Petrov, A.V., Slavin, G.A. (1962) Automatic welding of thin-sheet steel by a pulsed arc in argon. *Svarochnoye Proizvodstvo*, **2**, 6 – 9.
6. Paton, B.E., Potapievsky, A.G., Podola, N.V. (1964) Pulsed-arc consumable electrode welding with a programming control of the process. *Avtomaticheskaya Svarka*, **1**, 1 – 6.
7. Zaruba, I.I., Lebedev, V.K., Sheiko, P.P. *et al.* (1968) Welding with a modulated current. *Ibid.*, **11**, 35 – 40.
8. Esibyan, E.M. (1965) Semiconductor power source AP-2 for welding with a low-amperage pulsed-arc welding. *Ibid.*, **1**, 40 – 44.

INFLUENCE OF ANISOTROPY OF THE ROLLED STOCK MECHANICAL PROPERTIES ON INITIATION AND DEVELOPMENT OF TOUGH AND LAMELLAR-TOUGH FRACTURES

A.V. BERNATSKY
The E.O. Paton Electric Welding Institute, NASU, Kyiv, Ukraine

ABSTRACT

Brief description of expert estimations of service failures related to the structural texture, is given. The rationality of introduction of new terminology is presented in order to define the main kinds of lamellar fracture, namely lamellar-tough, lamellar-brittle, lamellar-fatigue and lamellar-hydrogen. A quantitative estimate of the influence of the percentage of sulphur in the base metal on the process of initiation and development of tough and lamellar-tough fractures, is given.

Key words: *anisotropy of mechanical properties, lamellar service fractures, investigations, crack resistance.*

Intensive studies in the field of application of the so-called pure steels for critical welded structures, were started in the E.O.Paton Electric Welding Institute of the NAS of Ukraine at the beginning of 1970s, together with I.P. Bardin TsNIIChermet. The fundamental studies of B.E. Paton, B.I. Medovar and other scientists working in this field [1 – 3], became widely applied in practice and were the next logical step in the sequential practical implementation of the ideology precisely defined already by E.O. Paton, which envisaged the use in welded structures of materials developed purposefully for specified service conditions taking into account the external impacts and meeting the requirements of welding technology.

However, despite certain achievements in this field, the possibilities for improvement of the purity of the structural steels which are welded, have by no means been exhausted.

The lamellar (laminated) cracks have been extensively discussed in the world publications. However, the main attention in this case was given to formation of lamellar cracks during welding. The influence of anisotropy and non-uniformity of service properties of steel rolled stock on the welded structure performance and fatigue life has not been considered just as broadly. Nonetheless, as was found during the investigations which formed the basis for this work, the influence of the mechanical properties anisotropy on cracking in welded structures in service, is a determinant factor in a number of cases.

Fractographic features of the sites of welded structure fracture due primarily to low mechanical properties across the thickness (so-called Z-direction) and service conditions, predetermined the rationality of introduction of new terms defining the main kinds of lamellar fracture, namely lamellar-tough, lamellar-brittle, lamellar-fatigue [4] and lamellar-hydrogen [5].

As the anisotropy of the mechanical properties of the steel sheet is largely determined by the texture of non-metallic inclusions and primarily, sulphides, this paper focuses on the influence of sulphur content in the base metal of welded structures on the causes for failures in service.

The aim of this paper is generalization of the results of expert evaluations of service failures and laboratory investigations related to the influence of sulphur on initiation of the tough and lamellar-tough fractures in welded structures.

It should be noted that we are dealing not with the widely known lamellar process cracks developing during welding, but with welded structure failures in service. Let us dwell on some of them in more detail.

Figure 1 shows the schematic of a completely fractured ammonia receiver, as well as its fragments. As a result of expert evaluation, it was found that the fracture site was in the zone of welding-on union P_5 of shell *1*. Sections with the so-called woody fracture were found in the fracture site, this being an indication of the lamellar-tough start of the tank fracture. Further on, under the impact of pneumatic loading, fracture propagated in shell *2* and was of brittle nature («chevron» pattern).

Scatter of fracture toughness values of shells *1* and *2* at above zero temperatures is noted by the results of Charpy sample tests. While for shell *1* these value are KCV^{+20} = 65 – 70 J/cm^2, for shell *2* — KCV^{+20} = 5.0 – 35.0 J/cm^2.

© A.V. BERNATSKY, 2000

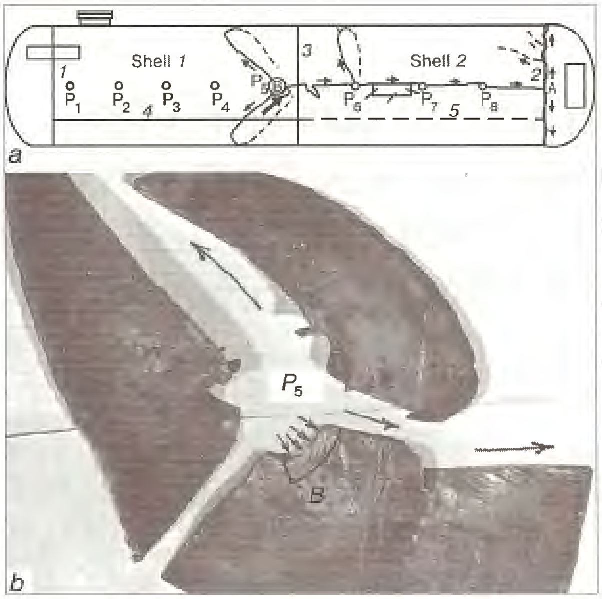

Figure 1. Diagram of a fractured ammonia receiver (*a*) and fracture fragments (*b*): B — fracture site (arrow shows the fracture propagation direction)

Therefore, low values of impact toughness of shell *2* promoted its brittle fracture, despite the lamellar-tough start of shell *1* fracture.

Figure 2, *a* shows the macrosection of the site of fracture of a welded structure, namely a refrigerating chamber of process equipment in «Che-

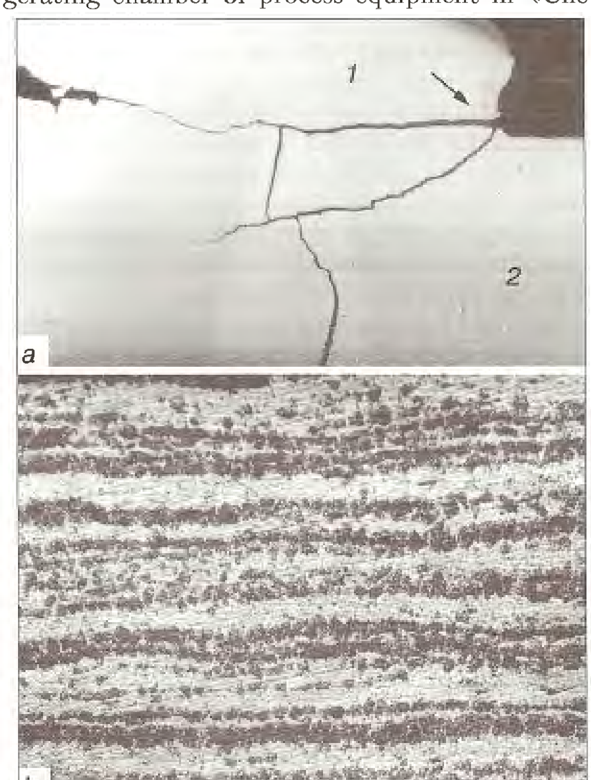

Figure 2. Lamellar-fatigue fracture of a refrigerating chamber: *a* — fracture site (shown by an arrow) (*1* — stiffener; *2* — cylindrical case of a drum); *b* — ferritic-pearlitic banding of base metal (×100) (reduced by 0.60)

Figure 3. Lamellar-fatigue fracture of a bridge framework: *a* — fracture site (*1* — stiffener; *2* — load-carrying beam); *b* — fracture site on a fragment (shown by an arrow)

Gevara» Nickel Works (Cuba). The chamber is a cylindrical rotating vessel filled with a bulky material. The vessel walls are reinforced with circular stiffeners in the form of individual sections. Crack initiation in the points of stiffener ending was detected in service.

Laboratory analysis revealed that the vessel was made of low-alloyed steel whose microstructure demonstrated a pronounced ferritic-pearlitic banding (Figure 2, *b*). Evaluation of the relative reduction in area φ_Z was performed on non-standard samples [6] of a small diameter (d_0 = 3 mm), because of the limited volume of the metal. In this connection, the derived values φ_Z = 10 % were considered to be somewhat overestimated. The base metal, because of its low mechanical properties across the thickness and a developed structural texture, was considered to be susceptible to lamellar cracking (GOST 28870–90), while the fracture was classified as lamellar-fatigue fracture by its fractographic features.

Figure 3 shows a fragment of a dismantled bridge framework structure. The cause for dismantling were cracks in the elements of the bridge structure, especially in the zones of stiffeners welding. The fracture site has a strongly «rubbed-in» plane-oriented section located parallel to the wall plane, which is a lamellar crack which initiated during welding and propagated under the conditions of cyclic loading, or a lamellar-fatigue crack formed directly in service as a result of the metal susceptibility to delamination and low cyclic viscosity across the thickness.

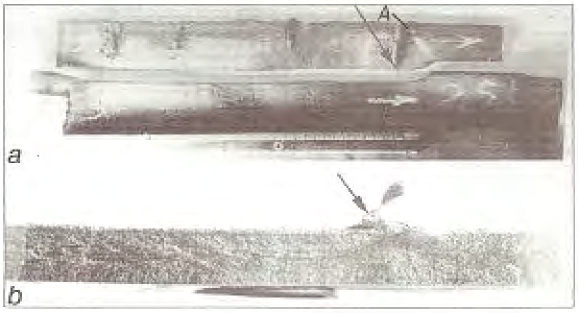

Figure 4. Fragment of a tank fracture: *a* — fracture site (A — side fillet weld); *b* — fracture site (shown by an arrow)

Characteristically, the surface of the section is 3 to 5 mm deeper than the wall surface and coincides with the location of the step on the fatigue fracture, this being indicative of an increased tendency to metal delamination in this zone. This case of fracture is mentioned in study [4].

Splitting of a 10 thous. m^3 tank occurred at the temperature of +4 °C during hydraulic testing after 13 h after the level of tank filling had reached 17.6 m. The fracture site was located in the 6th girder at the end of an unremoved side fillet weld (Figure 4). A brittle crack propagated to both sides for the total length of 375 mm, slowed down and further propagated in the tough mode. Presence of a comparatively soft raiser, a relatively high temperature at which fracture occurred, small thickness of the wall (7 mm) do not permit this fracture to be interpreted in terms of the traditional concepts.

It is important to emphasize that the characteristic «step-recess» in the site of the considered fracture suggests that the anisotropy of the mechanical properties has by no means the smallest role in initiation of this fracture.

Visual inspection of welded joints and components of crane trusses in the Magnitogorsk Metallurgical Works revealed a large number of lamellar cracks characteristic for such a type of welded joints (Figure 5, *a*). Cracks were mostly found in the shop columns made of 16G2AF steel, as well as the connections of the footing-crane beam made of 14G2AF steel. As shown by laboratory investigations, fractures are related to very low properties of ductility (φ_Z = 6.6 %) and toughness (KVC^{+20} = 7 – 8 J/cm^2) in *Z*-direction, which resulted from a high content of sulphides in the base metal (Figure 5, *b*). It should be also noted that the cracks propagated under the influence of cyclic loads arising from the crane movement.

All this pertains equally to lamellar fractures of the crane beams in the city of Krivoj Rog.

The critical condition of welded connections of off-shore platforms (city of Klaipeda) was related to a large number of structural lacks-of-penetration which in a number of cases gave rise to cracks propagating into the base metal. Laboratory investigations demonstrated that the base metal (X60,

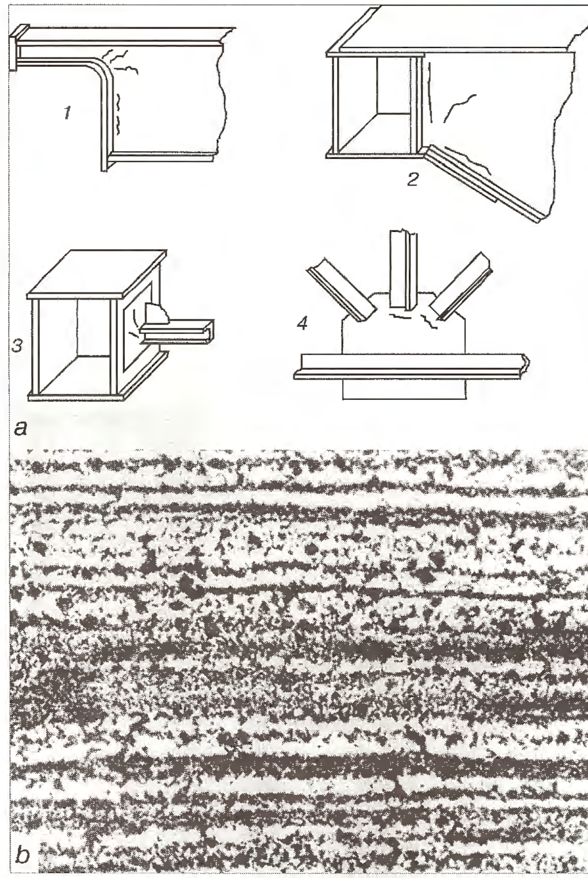

Figure 5. Lamellar fractures of welded components: *a* — kinds of welded components and areas of the most frequent cracks (*1* — support assembly of an end beam of a bridge crane; *2* — locations of abutting of the main and end beams; *3* — places of attachment of movement mechanism brackets; *4* — places of attachment of posts and braces); *b* — location of sulphides (×100) (reduced by 0.60)

24 mm thick) has low fracture toughness values across the thickness at low temperatures, which may lead to development of unstable fractures, especially under the conditions of low service temperatures.

It should be noted that in this case, lowering of fracture toughness in *Z*-direction is not related to the presence of sulfides, but is the consequence of a developed crystallographic texture. This issue is discussed in greater detail in [7].

Expert analysis of the lamellar-tough crack which caused a railway accident in the region of the city of Ufa, was performed to derive information on the causes for the product pipeline failure.

Figure 6. Fragment of the site of lamellar-tough fracture of a product line

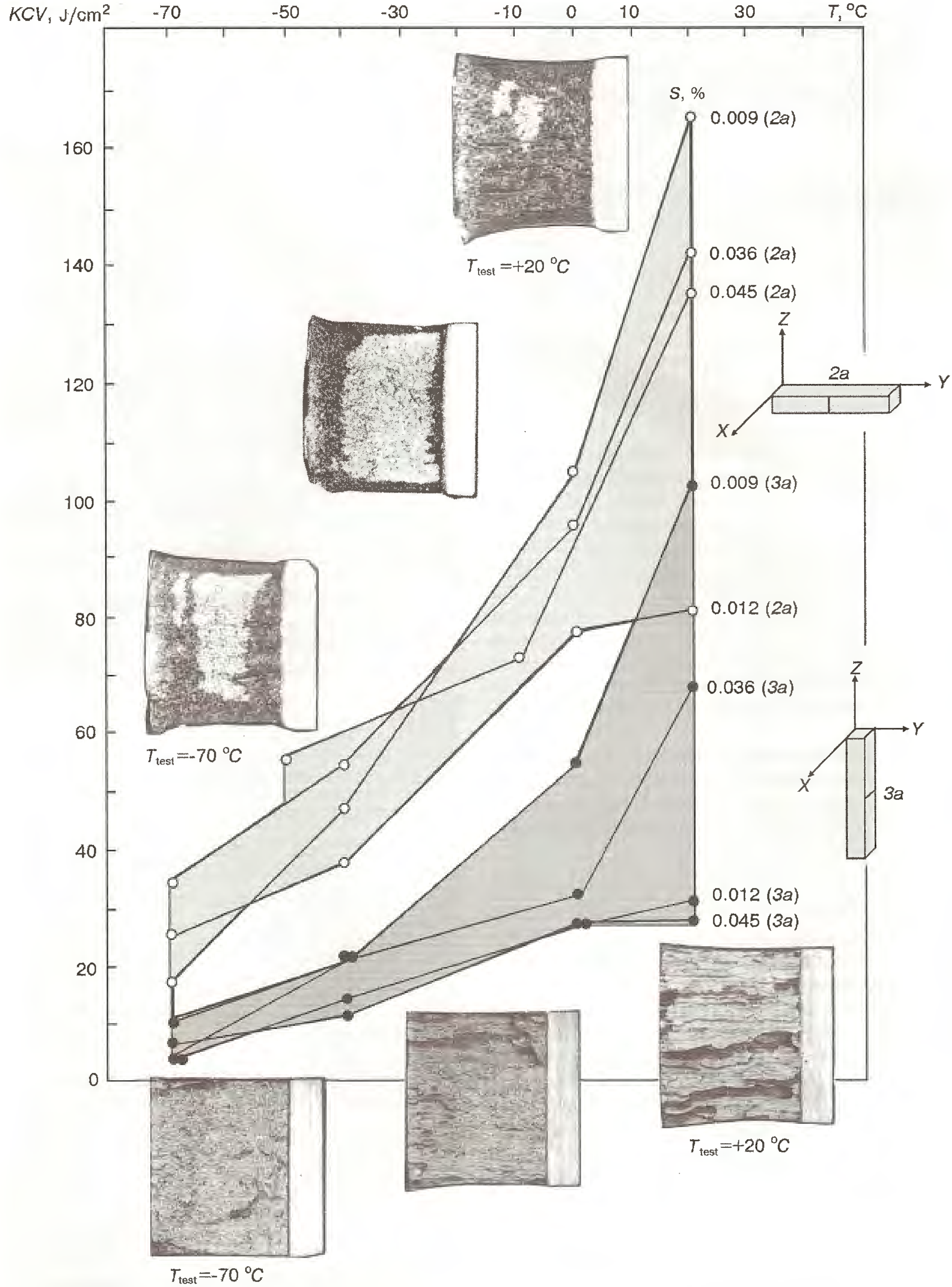

Figure 7. Results of impact bend testing of structural steels with different content of sulphur and characteristic fractographic features of fractures, depending on the sample position in space and temperature: *2a*, *3a* — sample location in the plate plane and *Z*-direction, respectively

Table 1. Composition of the tested steels, wt.%

Steel grade, thickness, mm	*C*	*Si*	*Mn*	*Cr*	*Ni*	*V*	*Cu*	*P*	*S*
09G2S, 35	0.050	0.670	1.30	0.10	0.02	0.02	0.05	0.017	0.045
16G2AF (Sh), 40	0.168	0.407	1.44	0.05	0.05	0.08	0.05	0.013	0.009
14G2AF, 35	0.152	0.380	1.25	0.05	0.05	0.07	0.05	0.012	0.012
14G2AF, 40	0.200	0.450	1.67	0.17	0.09	0.16	0.02	0.030	0.036

The crack shown in Figure 6 initiated one year before in the section where later on the rupture leading to the accident, occurred. The crack was located in the end section of the pipe (17G1S steel) highly contaminated by textured non-metallic inclusions (sulphides). A detailed analysis leads to the conclusion that the opening and, accordingly, stable propagation of the crack occurred during welding of a circumferential butt joint and subsequent service.

One of the principal and the most dangerous kinds of fracture of process equipment of petrochemical productions, is the lamellar-hydrogen cracking, and for furnaces an intensive layer-by-layer corrosion the appearance of which is related to the presence of sulphides in the base metal.

The hazard of this kind of fracture consists in weakening of the thickness of the net section of the structure, which, ultimately (considering the high rates of the base metal saturation with hydrogen) may lead to its local or total failure. Some aspects of this kind of fracture were discussed in [5].

In view of the limited scope of this paper, quite a large number of service failures related in some way to the anisotropy of the rolled metal mechanical properties did not get our attention. A large scope of laboratory investigations of structural steels and their welded joints with different physico-mechanical properties, namely St.3, 09G2S, 09G2SSh, 14G2AF, 14G2AFSh, 16G2AF, 16G2AFSh, 10KhSND, 12KhGDAF, 17GS, 17G1S, X60, X70, has been conducted, in order to determine the regularities of initiation of the tough, lamellar-tough and, later on, lamellar-hydrogen fractures. The content of sulphur varied between 0.001 (for X70 steel of controlled rolling, 24 mm thick) and 0.061 % (for 16G2AF steel 40 mm thick, with nitride strengthening). The derived results were the basis for GOST 28870–90.

In order to determine the characteristics of ductility and toughness of the studied steel grades, testing of standard and non-standard (including full-scale) samples was conducted in a broad range of temperatures (+500 to −196 °C) and different positions in space [4, 6, 8].

Study [4] and Figure 7 give the results of impact bend testing of low-carbon steel grades with different structural texture and the most characteristic fractographic features of the tough, brittle, lamellar-tough and lamellar-brittle fractures.

The composition and mechanical properties are given in Tables 1, 2. Appropriate graphical dependencies were plotted by the results of the conducted tests (Figure 8) for comparison of sulphur content in the metal and ductility and fracture toughness characteristics. For the impact bend tests, the value of critical crack opening displacement δ_c is plotted on the abscissas axis.

Calculation of value δ_c for each specific case was performed by the following formula:

Table 2. Mechanical properties of the tested steels

Steel grade, thickness, mm	*Sample location*	*Tensile testing*				*Impact bend testing, J/cm², at T, °C*				*δ_c, mm*	*S, %*
		σ_y, MPa	*σ_t, MPa*	*δ, %*	*ψ, %*	*−70*	*−40*	*0*	*+20*		
14G2AF, 35	Standard location	51.50	61.59	29.65	65.7	253	370	783	806	0.060	0.012
	Z-direction	41.26	58.25	87.00	12.9	65	145	275	305	0.020	
16G2AF (Sh), 40	Standard location	43.55	58.05	25.30	69.6	180	476	1033	1643	0.147	0.009
	Z-direction	40.94	56.78	26.40	42.4	60	210	530	1020	0.090	
09G2S, 35	Standard location	40.50	49.36	31.75	76.3	545	725	1740	1340	0.240	0.045
	Z-direction	34.90	47.63	27.45	32.0	85	120	275	280	0.020	
14G2AF, 40	Standard location	40.10	57.76	33.70	70.2	343	540	946	1420	0.125	0.036
	Z-direction	38.80	53.56	15.30	48.2	106	220	320	680	0.065	

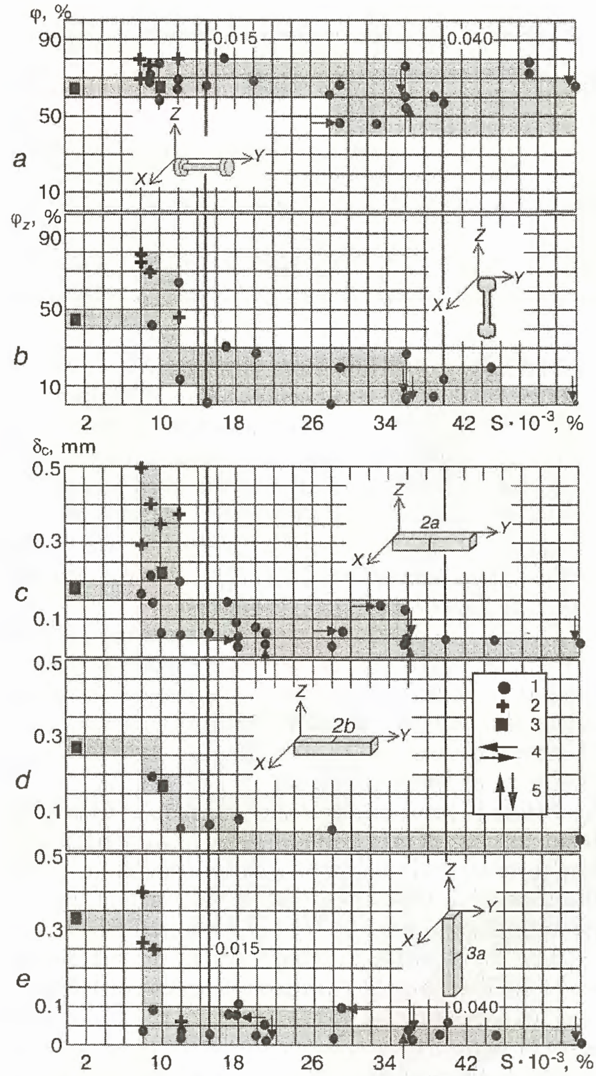

Figure 8. Dependence of reduction in area φ (*a*, *b*) and critical crack opening displacement δ_c (*c*, *d*) on sulphur percentage in the metal: *1* — low-alloyed hot-rolled steels; *2* — hot-rolled steels with a fixed temperature of the end of rolling; *3* — steels of controlled rolling; *4* — fracture of petrochemical equipment; *5* — fracture of welded structures

$$\delta_c = K\,\frac{KCV^{+20}}{\sigma_y}, \quad K = 0.75\,\frac{\sigma_y/\sigma_t}{1 + 0.33\,\sigma_t/\sigma_y},$$

where σ_y is the yield point; σ_t is the ultimate strength; KCV^{+20} is the impact toughness of Charpy samples at T_{test} = +20 °C; K is the proportionality factor.

Note that only the results derived in tough and lamellar-tough fracture of samples, were taken into account.

It should be borne in mind that the structural steel crack resistance depends on a whole range of characteristics. So, for steels of controlled rolling (X60, X70, etc.) the low values of fracture toughness across the thickness are related to the developed crystallographic texture [6, 9].

When the derived dependencies are considered, one can see regularities which, in our opinion, are of certain engineering interest in terms of selection of steels for service under the conditions of possible development of lamellar fracture.

First of all, it should be noted that in tensile testing of samples located in the plate plane, practically no lowering of the ductility characteristics is found with the increase of the amount of sulphur (Figure 8, *a*). When *Z*-samples (GOST 28870–90) are subjected to tensile testing, an abrupt lowering of the ductility characteristics occurs at S > 0.012 % (Figure 8, *b*).

When samples located in the rolling plane (Figure 8, *c*) are tested by impact bending, as well as in keeping with GOST 28870–90 (Figure 8, *e*, samples are located in *Z*-direction), lowering of fracture toughness values proceeds at S > 0.010 %. In the first case we are dealing with tough, and in the second case with lamellar-tough fracture.

Figure 8, *d* gives the results of impact bend testing of samples with a notch located on the plate surface (*2b*).

Despite the fact that the number of structural steels tested in such a manner, is relatively small, in this case also a certain tendency to lowering of the toughness values is observed at sulphur content S > 0.010 %.

At that time, the results of these tests were the basis for TU 14-1-4329–87, «Rolled stock of plate steel of 09G2SD and 12KhGDAF grades for welded metal structures of off-shore platforms» specifying the content of sulphur in the metal experiencing stresses across the thickness in service (*Z*-steels). Sulphur content in steels of this class should not exceed 0.010 – 0.015 %. The cases of lamellar fractures of welded structures mentioned above, are marked in Figures 8, *a* – *e*, as an illustration.

In keeping with the current standards for structural steels most often used in welded structures, the sulphur content in the metal is limited and is equal to 0.035 – 0.040 %. As is seen from Figure 8, such a condition is insufficient for resistance to lamellar fracture, and steels with sulphur content above 0.012 % can be regarded as susceptible to lamellar cracking under certain conditions of service.

This statement can be true in some degree, for steels exposed to aggressive media containing hydrogen sulphide and prone to lamellar-hydrogen cracking.

Figure 8 *c*, *e* gives the results of testing steels with lamellar-hydrogen damage, namely microcracks, cracks and «blowholes».

Despite the acceptability of the derived results in terms of the concepts being developed (sulphur content in the tested steels being 0.018, 0.029, 0.033, i.e. S > 0.012 %), one should admit that the steels susceptibility to lamellar-hydrogen cracking depending on sulphur content in the metal, has not yet been sufficiently well studied.

CONCLUSIONS

Analyzing the results of investigations of structural steels with different content of sulphur, it can be stated that the values of ductility in Z-direction and of toughness in the plate plane and across the thickness, essentially depend on sulphur content in percent in the base metal.

From this view point, it appears rational to select steels with sulphur content $S < 0.012$ % for the welded structures whose working sections can experience stresses across the thickness.

REFERENCES

1. Paton, B.E., Medovar, B.I., Semenov, S.E. *et al.* (1974) On the rationality of fabrication of critical welded structures of plate metal improved by ESR method. In: *Refining remelting*. Kyiv: Naukova Dumka.
2. Paton, B.E., Medovar, B.I., Semenov, S.E. *et al.* (1974) Electroslag remelting in steel plate production. *Ibid*.
3. (1983) *Electroslag technology*. Ed. by B.E. Paton, B.I. Medovar. Kyiv: Naukova Dumka.
4. Girenko, V.S., Bernatsky, A.V. (1987) Lamellar, lamellar-brittle and lamellar-tough fracture of welded joints. *Problemy Prochnosti*, **3**, 70 – 76.
5. Girenko, V.S., Rabkina, M.D., Bernatsky, A.V. *et al.* (1998) Some results of technical diagnostic of vessels and pipelines in petrochemical industry. *Tekhn. Diagnostika i Nerazrush. Kontrol*, **3**, 17 – 24.
6. Girenko, V.S., Bernatsky, A.V., Kozachek, V.M. (1991) Brittle fracture of steel with a developed crystallographic texture. *Avtomaticheskaya Svarka*, **1**, 6 – 9.
7. Girenko, V.S., Bernatsky, A.V., Dyadin, V.P. (1990) Static strength of cruciform welded joints at low temperatures. *Ibid.*, **2**, 28 – 32.
8. Girenko, V.S., Bernatsky, A.V., Kozachek, V.M. (1988) On unification of the methods of mechanical testing of rolled steel across the thickness. *Zavod. Laboratoria*, **11**, 74 – 79.
9. Usov, V.V., Girenko, V.S., Rabkina, M.D. et al. (1993) Influence of crystallographic texture on the anisotropy of fracture characteristics of low-alloyed steel of controlled rolling. *Fiz.-khim. Mekhanika Materialov*, **2**, 47 – 52.

HYGIENIC EVALUATION OF PROCESS OF ARC METALLIZING WITH FLUX-CORED WIRE OF Fe–B–Cr–Ni ALLOYING SYSTEM

G.A. KIRILYUK and **O.G. LEVCHENKO**
The E.O. Paton Electric Welding Institute, NASU, Kyiv, Ukraine

ABSTRACT

Quantitative characteristics of aerosols evolution in flux-cored wire arc metallizing of alloyed alloys are determined and recommendations are given on protection of workers and environment.

Key words: *flux-cored wire, metallizing, hygiene, ventilation, air.*

Electric arc flux-cored wire metallizing makes it possible to produce the alloyed wear-resistant coatings and it is characterized by a comparatively high efficiency. However, when using this method the losses in electrode material are comparatively high and can amount to 30 % [1 – 4]. The stream of a welding aerosol is formed when the air flow at 30 – 60 m^3/h consumption comes in contact with an electrode metal [2]. Main alloying elements are most often the following: carbon, chrome, nickel, manganese, molybdenum, aluminium, which, in welding aerosol composition, may be hazardous for the personnel and environment.

The present work is aimed at the determination of the level of evolutions and chemical composition of a hard constituent of the welding aerosol (HCWA) and at issue of recommendations for improving the labour conditions and environment protection.

The procedure of investigation is as follows. Metallizing was performed with experimental flux-cored wires (Table 1) in the OB-1286 installation, whose chamber and feeding mechanisms were equipped additionally with a head for an arc flux-cored wire metallizing. The chamber can remove air with aerosol with a rate of 10 – 15 m/s that occurs before the feeding of a working gas at pressure of 0.5 – 0.6 MPa. The conditions are as follows: current 200 – 250 A, arc voltage 20 – 23 V.

The total volume of HCWA determined as a difference in masses of a consumed wire and materials in the form of a precipitation in the chamber and on a filter of a suction system, was expressed by two characteristics: intensity of HCWA formation and a specific evolution. Samples of HCWA were selected with the help of filters FPP-15, set in an exhausting channel. Chemical analysis of samples was made using a generally-accepted procedure [3].

It was established that HCWA contains compounds of hexavalent and trivalent chromium, nickel, manganese, iron and others (Table 2).

The substances of the first class: hexavalent chromium and nickel are most hazardous for the health of the personnel [4]. Manganese which is introduced in this experiment from the wire sheath belongs to the second class of hazard, while trivalent chromium and iron belong to the third class.

The intensity of HCWA formation was 12.1 – 15.5 g/min (Table 3), and the specific evolutions – 90.7 – 116.3 g/kg of wire, that is by one order higher than in arc flux-cored wire welding [5]. The lowest HCWA evolution was observed when the nickel-free flux-cored wire was used for metallizing (the mass of evolutions of HCWA was

Table 1. Composition of experimental flux-cored wires, %

Wire components	*No. 1*	*No. 2*	*No. 3*
Sheath, steel 08 rimmed	75.0	75.0	75.0
Ferrochrome, FKh650	12.0	4.0	6.0
Chromium, Kh98.5	–	5.0	–
Nickel, PNE	3.0	–	3.0
Molybdenum, MPCh	2.0	2.0	2.0
Aluminium, PA-1	4.0	4.0	4.0
Master alloy, FKhB-1	–	10.0	–
Iron, PZh-1	4.0	–	10.0

Table 2. Mass share of HCWA components during flux-cored wire metallizing, %

Component	*No. 1*	*No. 2*	*No. 3*
Hexavalent chromium	0.32	0.05	0.19
Trivalent chromium	2.50	4.30	2.30
Nickel	2.70	–	2.30
Manganese	1.30	0.90	1.90
Iron	51.80	42.10	63.50
Other components	41.38	52.65	29.82

© G.A. KIRILYUK and O.G. LEVCHENKO, 2000

Table 3. Intensity of formation (V_e) and specific evolution (G_e) of HCWA

Component	No. 1		No. 2		No. 3	
	V_e, g/min	G_e, g/kg	V_e, g/min	G_e, g/kg	V_e, g/min	G_e, g/kg
HCWA	15.50	116.30	12.10	90.70	14.30	110.50
Including:						
hexavalent chromium	0.05	0.37	0.01	0.05	0.026	0.20
trivalent chromium	0.30	2.91	0.52	3.90	0.33	2.54
nickel	0.42	3.14	–	–	0.30	2.50
manganese	0.20	1.51	0.11	0.82	0.27	2.10
iron	8.03	60.24	5.09	38.18	9.08	70.17
other components	6.50	18.13	6.37	47.85	4.26	32.95

Table 4. Required air exchange of ventilation (Q) and content of harmful substances (C) in the working zone air

Component, LAC	No. 1		No. 2		No. 3	
	Q, m^3/kg	C, mg/m^3	Q, m^3/kg	C, mg/m^3	Q, m^3/kg	C, mg/m^3
Hexavalent chromium, 0.01	37000	None	4500	None	20000	None
Trivalent chromium, 1.00	2900	0.73	3900	0.30	2500	0.30
Nickel, 0.05	63000	0.05	–	None	50000	0.04
Manganese, 0.20	7500	0.08	4000	0.04	10000	0.04
Total air exchange	63000	–	4500	–	50000	–

12.1 g/min). Here, the evolutions of a hexavalent chromium were lower, while those of a trivalent chromium were higher. The presence of nickel (powder) in other wires contributes, evidently, to the formation of a hexavalent chromium, i.e. degree of its oxidation is increased.

The degree of toxicity of aerosols is characterized to a certain extent by an amount of air, required for the dilution of the harmful substance to a limiting admissible concentration (LAC). When wire No. 2 is used for the metallization the required air exchange should be 13 times less than that for the wire No. 1, which contains chromium.

The amount of harmful elements in air of the working zone was evaluated under the industrial conditions during restoration using the flux-cored wire metallization in the installation UD-209 equipped with a special ventilation box. The data of measurements (Table 4) did not exceed the admissible values.

The design of ventilation and protection systems in the arc metallizing is mainly based on the fact that HCWA is concentrated mainly in a high-speed air stream of a definite direction, therefore the best results were obtained using housing for trapping the direct and reflected HCWA-containing air streams. The contaminated air was purified usually by using separators with water, cyclones and other systems for the dust trapping [6].

Thus, the installations for metallizing should be equipped with an effective local ventilation [7], and a production room with a general exchanged ventilation [6] designed for a partial removing the aerosols entered from the metallizing installations. If the ventilation cannot decrease the content of harmful elements in air of the working zone to LAC, then it is necessary to use the means of an individual protection of the respiratory organs [7].

CONCLUSIONS

1. Hygienic characteristic of air of the working zone during the arc flux-cored wire metallizing is determined by the HCWA composition and the efficiency of the exchange ventilation.

2. Air contamination with a metallic dust and HCWA is relatively high that causes the installation equipping with a system for its purification.

REFERENCES

1. Khasuy, A. (1975) *Technique of spraying*. Moscow: Mashinostroyeniye.
2. Krechmar, E. (1966) *Spraying of metals, ceramics and plastics*. Moscow: Mashinostroyeniye.
3. (1990) *Methodical recommendations on determination of harmful substances in welding aerosol (hard phase and gases). No. 4549–88*. Moscow: Minzdrav USSR.
4. Knudsen, I., Stern, R. (1980) Assaying potential carcinogenicity of welding fume and hexavalent chromium with the mammalian spot test. In: *Proc. of Colloquium on Welding and Health of Commission of IIW*.
5. (1976) *Methodical recommendations on prevention of diseases in workers in using new methods of welding and surfacing with new welding consumables*. Kyiv: Minzdrav UkrSSR.
6. Pisarenko, V.L., Roginsky, M.L. (1981) *Ventilation of working rooms in welding production*. Moscow: Machinostroyeniye.
7. Levchenko, O.G., Metlitsky, V.A. (1999) *New means of protection against welding aerosols*. Manual. Kyiv: Ekotekhnologia.